

# RSC Advances



This is an *Accepted Manuscript*, which has been through the Royal Society of Chemistry peer review process and has been accepted for publication.

*Accepted Manuscripts* are published online shortly after acceptance, before technical editing, formatting and proof reading. Using this free service, authors can make their results available to the community, in citable form, before we publish the edited article. This *Accepted Manuscript* will be replaced by the edited, formatted and paginated article as soon as this is available.

You can find more information about *Accepted Manuscripts* in the [Information for Authors](#).

Please note that technical editing may introduce minor changes to the text and/or graphics, which may alter content. The journal's standard [Terms & Conditions](#) and the [Ethical guidelines](#) still apply. In no event shall the Royal Society of Chemistry be held responsible for any errors or omissions in this *Accepted Manuscript* or any consequences arising from the use of any information it contains.

# Dynamic Imine Chemistry in Metal-organic polyhedra

Harsh Vardhan<sup>a,b</sup>, Akshay Mehta<sup>a,b</sup>, Ipsita Nath<sup>a,b</sup>, and Francis Verpoort<sup>a,b,c,d\*</sup>

<sup>a</sup>: Laboratory of Organometallics, Catalysis and Ordered Materials, State Key Laboratory of Advanced Technology for Materials Synthesis and Processing, Wuhan University of Technology, Wuhan, China.

<sup>b</sup>: Department of Chemistry, Chemical Engineering and Life Sciences, Wuhan University of Technology, Wuhan 430070, P.R. China.

<sup>c</sup>: National Research Tomsk Polytechnic University, Lenin Avenue 30, 634050 Tomsk, Russian Federation.

<sup>d</sup>: Ghent University, Global Campus Songdo, 119 Songdomunhwa-Ro, Yeonsu-Gu, Incheon 406-840, South Korea.  
Email: francis.verpoort@ugent.be

## Abstract

Schiff base ligands prepared by the condensation reaction of carbonyl compounds and amines possess an excellent chelating ability. The chemistry of imine bond formation is among the most robust dynamic covalent chemistries employed for the construction of metal-organic materials. This review highlights the intercession of these linkers in the preparation of self-assembled architectures mainly metal-organic polyhedra and highlights their role in various key applications.

**Keywords:** Aldehydes, Amines, Imines, Self-assembly, Metal-organic polyhedra.

## 1. Introduction

The condensation reaction between aldehydes and amines to yield imines has been known for almost one and a half centuries since its discovery by the German chemist Hugo Schiff in 1864.<sup>1</sup> The condensation product (Schiff base) has an azomethine group with a general formula (Figure 1),  $\text{RHC}=\text{N-R}'$  where R and R' are alkyl, aryl, cyclo alkyl, or heterocyclic group. The nucleophilic addition of an amine to a carbonyl compound gives an unstable carbinolamine, which subsequently undergoes acid catalyzed dehydration to form a stable imine molecule. This conversion of hemiaminal to imine *i.e.* the dehydration step is the rate determining step and the

whole reaction is catalyzed by acid as shown in figure 2. Yet, the acid concentration cannot be too high due to the basic nature of amines and since the protonated amine are non-nucleophilic, equilibrium is pulled to the left and carbinolamine formation cannot occur. Therefore, Schiff base syntheses are best carried out at mildly acidic pH.<sup>2</sup> Mechanistically, this reaction is somewhat analogous to the E<sub>2</sub> elimination of alkyl halides except it is not a concerted reaction. The dynamic imine bond is affected by substrate properties such as steric and electronic features, as well as external factors like temperature, solvent, concentration, and pH. In general, imines can participate in three types of equilibrium controlled reaction (Figure 3):

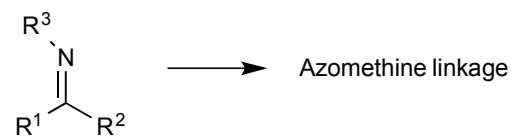
- (a) Hydrolysis – The imine reverts back to the precursor amine and carbonyl-containing compound (s) on addition of water.
- (b) Transimination – Upon introduction of second amine, the original imine may undergo transamination, resulting in the R group being exchanged.
- (c) Metathesis – Upon introduction of secondary imine, the two imines can undergo a reaction in which the two R group are exchanged.

Similar to imine formation, transimination also proceeds to the formation of tetrahedral intermediate (aminal) that subsequently decomposes to give a new imine and amine. The position of equilibrium depends on the relative basicities of the amines and is usually biased towards the formation of imine incorporating the most basic amine.<sup>3</sup> Transimination may be homotransimination (both amines are aliphatic or aromatic) and heterotransimination (one is aliphatic and other is aromatic) and influence by Brønsted and Lewis acids,<sup>4-6</sup> for instance, Sc<sup>III</sup> triflate salts catalyse the exchange reactions between sterically hindered imines, derived from 9-anthracenecarboxaldehyde, and several amines in chloroform. Sc(OTf)<sub>3</sub> accelerates the reaction up to five orders of magnitude compared to the uncatalysed process and up to two orders of magnitude compared to the proton catalyst<sup>7</sup>, in most favourable cases. Imine metathesis on the other hand, is a scrambling reaction between two performed imines which undergo exchange between their amine portions forming two new imines. Initially, Ingold and Piggot suggested a concerted mechanism of this reaction<sup>8,9</sup> and latter, a variety of transition metal complexes containing a metal-imido group M=NR (M = Zr, Mo, Nb, Ti, Ta) were used to catalyse the metathesis.<sup>10-16</sup> Recently, Stefano and Ciaccia critically discussed the mechanism operating in

imine chemistry in organic solvents and unambiguously explained the mechanistic aspects of hydrolysis, transimination, and metathesis reactions.<sup>17</sup>

The reversible condensation reaction between aldehydes and amines is one of the most ubiquitous reactions which define a discipline known as dynamic covalent chemistry (DCC), which is extensively employed in the construction of exotic molecule and extended structure.<sup>18-21</sup> Templated-directed synthesis and non-covalent interactions in conjunction with DCC led to the formation of a range of molecules including interlocked molecules. The inherent element of 'proof-reading' and 'error-checking' of such reversible reactions makes DCC an especially appealing strategy since it results, given enough time, in the formation of most thermodynamically stable product(s). This thermodynamic equilibrium is generally manipulated in one of the two ways: (i) the equilibrium can be driven in one direction by adjusting the reaction conditions, *i.e.*, adding or removing starting material (s) or product (s), or (ii) the starting material can be chosen so as to encourage the formation of the particular product, *i.e.*, by incorporating certain steric or electronic recognition features into the precursors which favour the formation of the desired product. Furthermore, imine type molecules such as oximes, hydrazones, phenylhydrazones, and semicarbazones synthesized from carbonyl compounds and mono substituted ammonia derivatives such as  $\text{NH}_2\text{-G}$  (where G has a  $-I$  group like  $-\text{OH}$ ,  $-\text{NH}_2$ , *etc.*) are very stable and hence cannot be easily hydrolyzed.

The presence of a lone pair in the  $\text{sp}^2$ -hybridized orbital of nitrogen atom of the azomethine group is of considerable importance. Because of the relative easiness of preparation, synthetic flexibility, presence of  $\text{C}=\text{N}$  group, excellent chelating group and the chelating ability is further augmented when nitrogen atom of azomethine linkage is present in the vicinity of one or more functional groups like  $-\text{OH}$  or  $-\text{SH}$  so as to form a stable five or six membered ring with the transition metal ions.<sup>22,23</sup> Metal-organic polyhedra are three dimensional discrete structures usually prepared by the self-assembly of metal ions and highly directional *m*-BDC or bis(pyridine) or exo-/endo-functionalized ligands or even imine linkers possessing suitable symmetric axis and point groups. This review summarizes the profound role of dynamic imine chemistry in the synthesis of self-assembled architectures mainly metal-organic polyhedra of various geometries and briefly highlights their application in bunch of areas.



R<sup>1</sup>, R<sup>2</sup> = Carbonyl compound part

R<sup>3</sup> = Amino part

Figure 1. Structure of azomethine group.

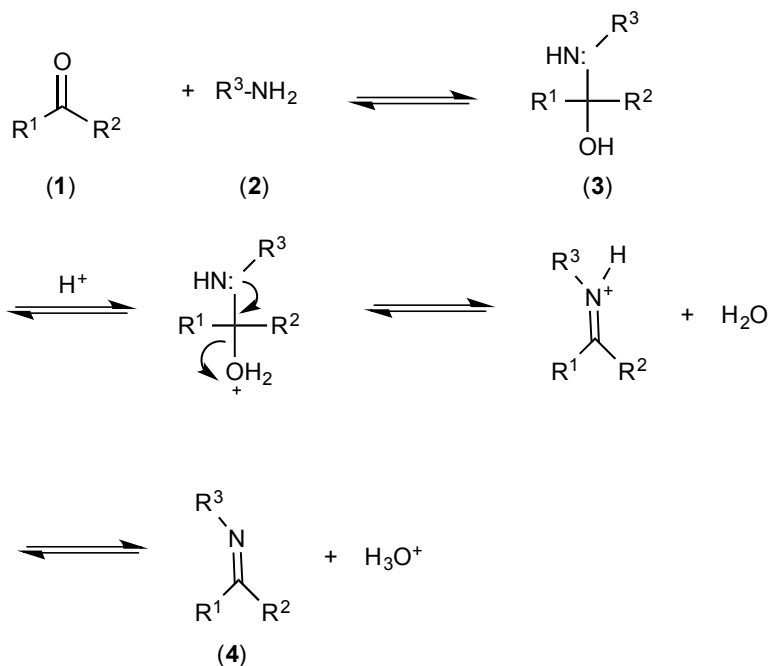


Figure 2. Rate determining step in the synthesis of Schiff base.

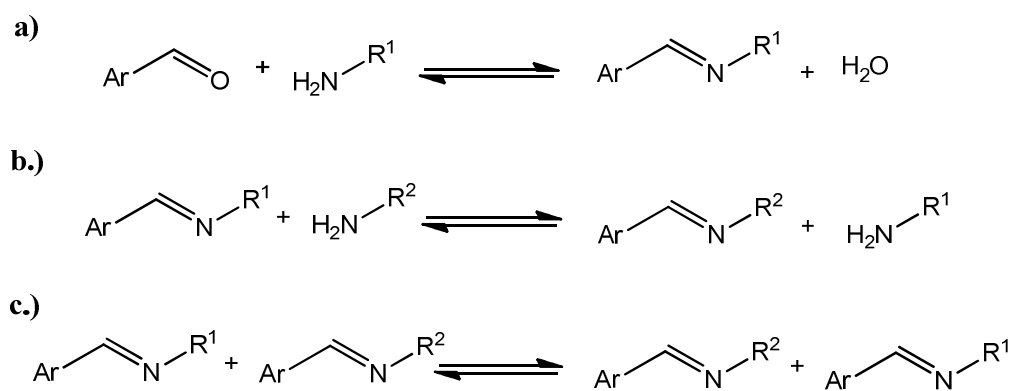


Figure 3. The three types of imine reactions (a) imine condensation, (b) transimination, and (c) metathesis.

## 2. Chelated Schiff Bases

The basic imine nitrogen exhibits  $\pi$ -acceptor properties and the presence of one or more donor groups in the proximity positively influences the chelating ability. Salen-type ligands are commonly used to specify ONNO-tetradentate bis-Schiff base prepared by the condensation of diamines derivative with  $\beta$ -diketone, *o*-hydroxy aldehyde or ketone (figure 4 structures 1-4).<sup>24, 25</sup> Moreover, the construct of Schiff base may involves symmetry elements and stereogenic centers, for instance, chiral copper-Schiff bases developed by Noyori in 1968 were employed in metal carbenoid cyclopropanation of styrene<sup>26</sup> for which he received in the 2001 the Noble prize in chemistry (figure 4, structure 6). Schiff base macrocycles prepared by the condensation of appropriate formyl- or keto- and amines have a range of functions in supramolecular and coordination chemistry.<sup>27</sup> They have a profound capability to stabilize metal ions (Lewis acid) in various oxidation states and thermodynamic aspects of their stability rely on the size, oxidation state of metal ions, nature of donor atoms, and five or six membered ring formation. Metal complexes of Schiff base have an unprecedented role in catalysis, for example, Co(II), Fe(III), and Ru(III) complexes were employed in oxidation of cyclohexane into cyclohexanol and cyclohexanone in presence of hydrogen peroxide<sup>28</sup> and Ru(II) Schiff base complexes are excellent catalysts for the olefin metathesis (figure 4, structures 5-8).<sup>29-32</sup> Binucleating complexes of Fe, Co, Ni, Zn with neutral bis(iminopyridyl)benzene and monoanionic bis(iminopyridyl)phenolate served as a catalyst in the oligomerization of ethylene. Lanthanide metal complexes with Schiff bases [LaL<sub>2</sub>(NO<sub>3</sub>)<sub>3</sub>], [CeL<sub>2</sub>(NO<sub>3</sub>)<sub>3</sub>], [PrL<sub>2</sub>(NO<sub>3</sub>)<sub>3</sub>], [NdL<sub>2</sub>(NO<sub>3</sub>)<sub>3</sub>], [SmL<sub>2</sub>(NO<sub>3</sub>)<sub>3</sub>], [GdL<sub>2</sub>(NO<sub>3</sub>)<sub>3</sub>], [TbL<sub>2</sub>(NO<sub>3</sub>)<sub>3</sub>], [DyL<sub>2</sub>(NO<sub>3</sub>)<sub>3</sub>], and [ErL<sub>2</sub>(NO<sub>3</sub>)<sub>3</sub>] demonstrate antibacterial activity against bacteria *Escherichia Coli* and *Bacillus subtilis*. Praseodymium and erbium complexes are highly active towards *E.coli*, whereas cerium, praseodymium, and erbium complexes were found to be active against *B. Subtilis*.<sup>33</sup> Furthermore, Schiff bases have been used as an effective corrosion inhibitor by forming a monolayer on the surface to be protected. The presence of C=N moiety in an inhibitor is responsible for chemisorption between the inhibitor and metal surface.<sup>34</sup> The azomethine group is able to form hydrogen bond at the active centers of cellular entities responsible for the interference in normal cellular phenomenon. An imine linkage between the aldehyde derived from vitamin A and the protein 'Opsin' in the retina of the eyes plays a crucial role in the vision.<sup>35</sup> Pyridoxalphosphate is a biologically important aldehyde and an active form of vitamin B6. It serves as a coenzyme by forming an imine with an amino acid and is involved

in transamination reaction leading to the transfer of the amino group from one amino acid to another which is indeed important for metabolism.<sup>36</sup>

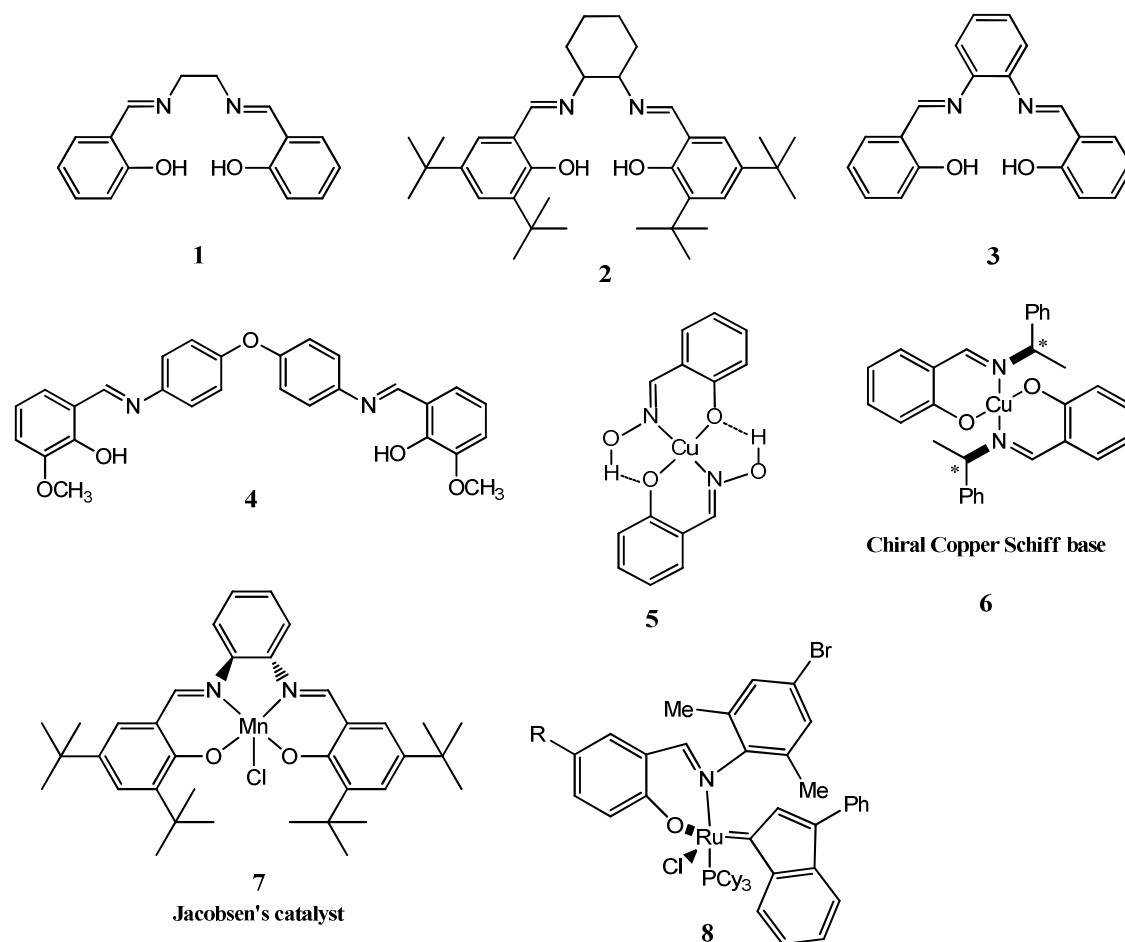


Figure 4. Salen type ligands (1-4) and Schiff base catalysts (5-8).

Self-sorting can be defined as the spontaneous reorganization of a disordered multicomponent system into a set of subsystems of fewer components with greater order.<sup>37, 38</sup> For this reason, self-sorting has emerged as a promising preparative method to enable the simultaneous synthesis of high-purity products from a complex mixture of starting materials. Osowska and Miljanić examined a [3×3] mixture consisting of three anilines and three aldehydes.<sup>39</sup> All nine possible imines were present at equilibrium; the first equivalent of I<sub>2</sub> effectively oxidizes the most-electron-rich imine to the oxidized product, benzimidazole. Depletion of the most-electron-rich imine essentially removes corresponding anilines and aldehydes from the reaction mixture as the system re-equilibrates to replace that imine. The second equivalent of I<sub>2</sub> will subsequently reduce the [3×3] mixture. Moreover, the same group

highlighted the self-sorting of the most complex experiment consisting of 25 imines originating from a [5×5] library constructed from five aldehydes and five amines.<sup>40</sup> A fascinating example of this is recently reported by Mukherjee *et al.* by reaction of three unsymmetrical aldehydes (A, B, and C) with a flexible triamine, **X**, tris(2-aminoethyl)amine.<sup>41</sup> The reaction of aldehyde **A** (3 eq) with amine (2 eq) in chloroform at room temperature for 24 h affords a single isomer of **A<sub>3</sub>X<sub>2</sub>**, where two imine functionalities orient in the same directions and one in reverse direction (**II**) rather than stereo isomer in which all similar aldehyde/imine functionalities are spatially oriented in the same directions (**I**) as shown in figure 5. Whereas, aldehyde **B** with triamine generated a mixture of **I** and **II** isomers however, vapour diffusion of *n*-pentane into a chloroform solution formed rod-shaped crystal of **B<sub>3</sub>X<sub>2</sub>** isomer **II** (Figure 4). Aldehyde **C** with triamine, on the other hand, affords a mixture of stereoisomers under the same set of conditions, and selective formation of one isomer is impossible. It is worth to mention that the energy difference between the isomers ( $\Delta H = 1.26, 1.37, \text{ and } 0.29 \text{ Kcal/mol}$  for aldehyde **A**, **B**, and **C** respectively) was the governing factor in isomer selection which correlates with the geometric shapes and size of reacting aldehyde.

Dynamic covalent imine chemistry in combination with templates allows the formation of topologically interesting molecules such as Borromean ring,<sup>42</sup> Solomon knots,<sup>43</sup> and other mechanically interlocked molecules like rotaxanes and catenanes.<sup>44, 45</sup> The presence of  $\pi$ -electron acceptor, bispyridinium template directs the synthesis of a cage-like macrobicycle by the reaction of 1,3,5-benzenetri-aldehyde and 2,2'-(ethylenedioxy)diethylamine in  $\text{CHCl}_3$ .<sup>46</sup>





[2]catenanes. Terephthaldehyde and 2,2'-(ethylenedioxy)diethylamine were mixed in 1:1 ratio along with tetracationic cyclobisparaquat in CD<sub>3</sub>CN to form [2]catenane albeit, no [2]catenane was formed if 1,5-diformylnaphthalene was employed instead of terephthaldehyde.<sup>47</sup> Unsymmetrical [2]catenane was synthesized as major product by reaction of 1,5-diformylnaphthalene and terephthaldehyde with diamines and cyclophane. In addition to  $\pi$ -templated dynamic imine assembly, hydrogen bonding mediated imine assembly has been extensively used by Stoddart and co-workers for the synthesis of rotaxanes.<sup>21</sup> [2]rotaxanes were obtained by mixing bis(3,5-dimethoxybenzyl)ammonium hexafluorophosphate with a solution of 2,6-pyridinedicarboxaldehyde and tetraethylene glycol bis(2-aminophenyl)ether. The imine formation is assisted by [N<sup>+</sup>-H $\cdots$ X] hydrogen bonding and [N<sup>+</sup>-C-H $\cdots$ X] (X = O or N) interactions as well as  $\pi$ - $\pi$  interactions between the dumbbell and the imine macrocycle.<sup>48</sup>

### 3. Imine Metal-organic polyhedra

In 1893, Alfred Werner explained the structure of octahedral transition metal complexes and provided the basis of assigning coordination number and oxidation state to what were then known as double salts.<sup>49</sup> This work was the beginning of modern coordination chemistry and significantly expanded the field of inorganic chemistry. In the last few decades, one of the important branches of coordination chemistry has emerged known as metal-organic polyhedra. Metal-organic polyhedra are three dimensional discrete structures, typically constructed by the self-assembly of metal ions and ligands having multiple binding sites and suitable symmetric axis. Geometry of discrete architectures prominently depends on the coordination geometry of transition or inner transition metal ions, highly symmetric flexible or rigid linkers candidly described by various parameters such as bend angle ' $\theta$ ', and nature of solvent.<sup>50</sup> These hollow molecular flasks possess inner cavity of appropriate volume and can be categorized into platonic, archimedean, faceted, and stellated polyhedra. Various research groups around the globe extensively used a wide range of approaches in the synthesis of polyhedra of complex topology. Out of various strategies developed using metal-ligand coordination, directional bonding, symmetry interaction, molecular paneling, weak link, and dimetallic building block are very common. These approaches are predominantly used by Atwood,<sup>51</sup> Cotton,<sup>52,53</sup> Fujita,<sup>54,55</sup> Lindoy,<sup>56-58</sup> Mirkin,<sup>59,60</sup> Nitschke,<sup>61-63</sup> Raymond,<sup>64-66</sup> Stang,<sup>67-72</sup> Saalfrank,<sup>73,74</sup> Ward,<sup>75,76</sup>

Yaghi,<sup>50,77-79</sup> Zhou,<sup>80-85</sup> and others<sup>86-91</sup> in designing 2D and 3D supramolecular architectures of various shapes. Three dimensional polyhedra microenvironment imposed by the inner space of molecules confers unique molecular recognition towards guests of appropriate size and shape. Furthermore, this encapsulation ability leads to a range of applications such as catalysis,<sup>92,93</sup> drug delivery,<sup>94-98</sup> and so on.<sup>99-102</sup> Self-assembled processes exploiting dynamic imine bond (C=N) and coordinative N→M bonds to connect multiple precursor units are unprecedented and are an extension of various approaches highlighted above to form highly complex 2D and 3D structure of particular geometry.<sup>103, 104</sup>

Warmuth *et al.* used diversified  $C_4$ -symmetric cavitand derivatives having ethylene and propylene spacers with a conical angle of  $85.4^\circ$  and  $93.7^\circ$  between two opposite aryl units carrying an aldehyde group. The [6+12] condensation reaction of ethylene spacer cavitand with rigid 1,1'-biphenyl-4,4'-diamine and *p*-phenylenediamine formed 24 imine bonds and afforded  $M_6L_{12}$  nanometer octahedrons.<sup>105</sup> The other cavitand derivative with similar conical angle condensed with the more flexible ethylenediamine to generate achiral  $M_4L_8$  product. The rigidity of the diamine and the angular aspect of cavitand play a prominent role in directing the outcome of the possible architectures. Gawronski and co-workers highlighted the preparation of a tetrahedral cage from the [4+6] condensation reaction between 1,3,5-triformylbenzene and 1,2-diaminocyclohexane.<sup>106</sup> Moreover, Cooper's group used the same carbonyl compound for the synthesis of a tetrahedral cage by reaction with 1,2-diamines such as 1,2-ethylenediamine and 1,2-propylenediamine.<sup>107</sup> The high yield of stable metal-organic capsules from the one-step imine formation exemplified the robust nature of this new dynamic covalent chemistry approach in the assembly of preorganized units.

### 3.1 Tetrahedral Imine Metal-organic polyhedra

A tetrahedron, the simplest of the platonic solids, can be assembled using a few different metal-ligand stoichiometries, first,  $M_4L_6$  tetrahedra, where the four metal ions occupy the vertices and the six ligands acts as an edges, second,  $M_4L_4$  tetrahedra, where the metal ions act as the four vertices, and the four faces of the tetrahedra are spanning by ligands with 3-fold symmetry, and third,  $M_6L_4$  tetrahedra or truncated tetrahedra, where the ligands occupying each of the four faces of the tetrahedron are connected by metal centers on the middle of the edges.

Nitschke and co-workers designed  $M_4L_6$  tetrahedral cage utilizing dynamic covalent and coordinative bond in tandem from multicomponent systems. The synthesis of tetrahedral cage was achieved by treatment of 2-formyl pyridine (**C1**, figure 6) and 4,4'-diaminobiphenyl-2,2'-disulfonic acid (**A6**, figure 10) with iron (II) in presence of base<sup>108</sup> (Figure 7), where four Fe(II) vertices were connected by six bis-bidentate ligands, each containing two chelating pyridyl-imine units. The symmetric tetrahedral cage has an extraordinary stability due to the presence of iron(II) in the low spin state and strong binding with the imine ligand (covalent C=N and coordinative N→Fe). The symmetrical arrangement of sulfonate groups on the periphery of the cage is responsible for its high water solubility ( $34\text{gL}^{-1}$ ). This anionic cage has high selectivity for appropriately sized cyclohexane and cyclopentane over similar sized organic cations or alcohols. Interestingly, addition of tosylic acid (variation of pH) or chelating tris(2-ethylamino)amine disassembles the cage and drives the formation of a mononuclear iron complex both enthalpically and entropically, whereas addition of base reassembled the anionic cage.<sup>108</sup> This fascinating encapsulation behaviour was further exemplified by means of a Diels-alder reaction between furan and maleimide in presence of benzene as a competitive guest,<sup>109</sup> stability of unstable pyrophoric white phosphorous,<sup>110</sup> and encapsulation of most effective greenhouse gas  $\text{SF}_6$  ( $K_a = 1.3 \times 10^4 \text{ M}^{-1}$ ) over Ar,  $\text{N}_2$ , Xe,  $\text{CO}_2$ , and  $\text{N}_2\text{O}$ .<sup>111</sup> The same imine ligand also self-assembled with copper and nickel ions to form analogue  $M_4L_6$  tetrahedral cages. Structurally, cobalt and nickel cages are similar to  $[\text{Fe}_4\text{L}_6]^{4-}$  cage, but have a longer M-M bond length (Fe-Fe=12.83 Å, Ni-Ni=13.03 Å, and Co-Co=13.04 Å) which, in turn, positively influenced the cavity size and opens the host-guest interactions to a larger extent.<sup>112</sup> The internal cavity volume of the cobalt tetrahedral cage is  $149\text{-}153\text{Å}^3$  susceptible enough for encapsulation of a range of guests such as cycloheptane, cyclooctane, methylcyclohexane, 2,3-dimethylbutane, *n*-hexane, and toluene albeit, large size *n*-heptane and cyclodecane did not show any host-guest interactions. The reason for such selective encapsulation behaviour is the larger ionic radii of the high spin  $\text{Co}^{\text{II}}$  (0.745 Å) as compared to the low spin  $\text{Fe}^{\text{II}}$  (0.61 Å) leading to longer M-L bonds and a greater ability of the ligands to dynamically adopt a wide range of torsion angles. Furthermore,  $[\text{Fe}_4\text{L}_6]^{4-}$  cage catalytically influenced the reaction of furan with singlet oxygen photogenerated by methylene blue to form high energy endoperoxide intermediate transformed into fumaraldehydic acid. 1,4-addition of nitromethane to fumaraldehydic acid in the presence of

L-proline formed cyclized product which on subsequent reduction by  $\text{NaBH}_4$  afforded lactone in 46% yield.<sup>113</sup>

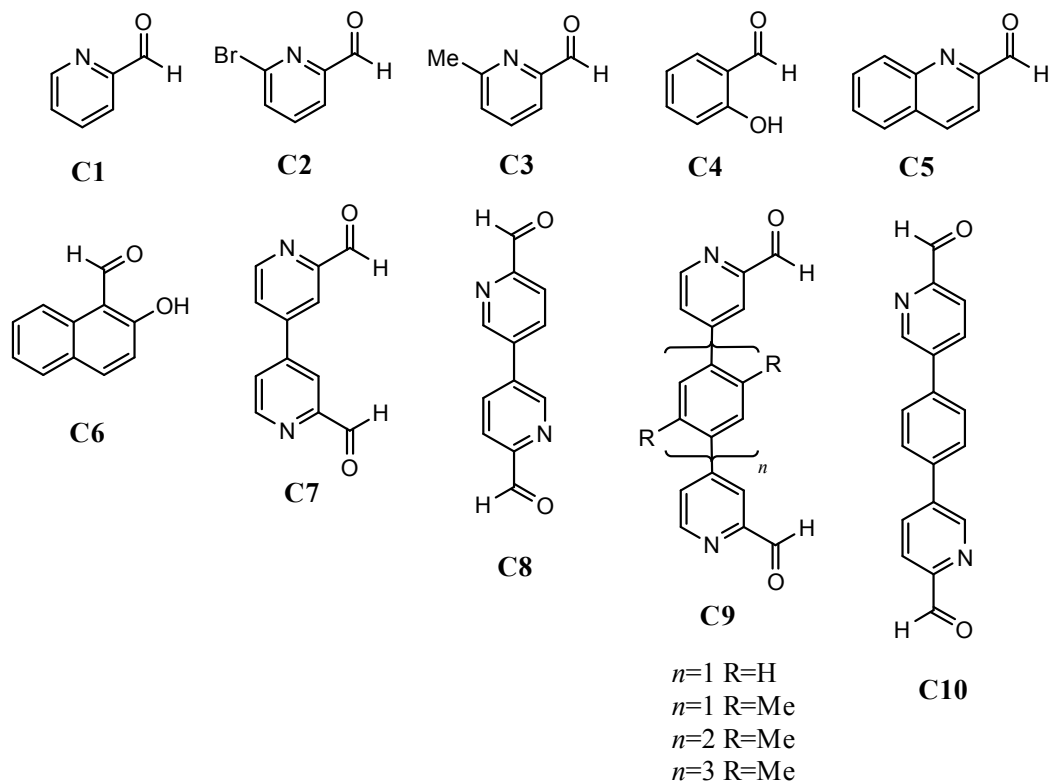


Figure 6. List of carbonyl compounds (C1-C10).

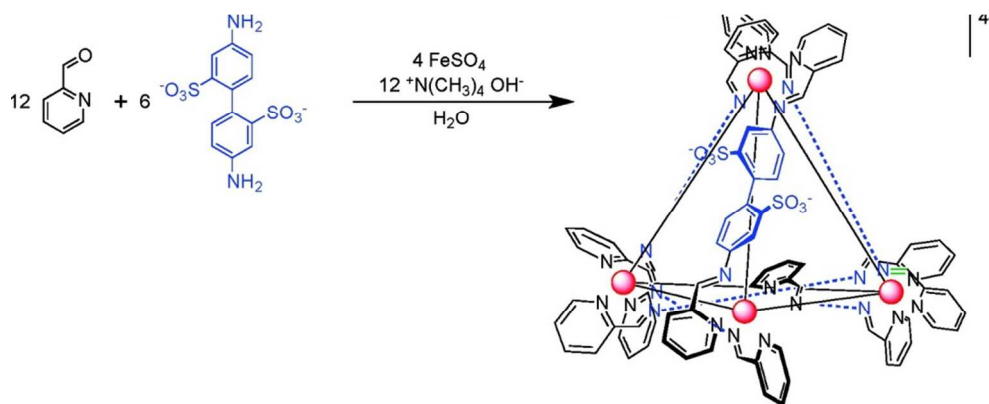


Figure 7. Subcomponent self-assembly of  $[\text{Fe}_4\text{L}_6]^{4+}$  cage. Adapted from ref.108 (Copyright ©2008 Wiley-VCH Verlag GmbH & Co. KGaA, Weinheim).

Diaminoterphenyl (**A7-A10**) condensed with 2-formylpyridine (**C1**) to form imine which on reaction with  $\text{Fe}^{\text{II}}$  ions in acetonitrile afforded  $[\text{Fe}_4\text{L}_6]^{8+}$  tetrahedral cage.<sup>114</sup> The positively charged cage may have homochiral  $T$  ( $\Delta\Delta\Delta\Delta / \lambda\lambda\lambda\lambda$ ), achiral  $S_4$  ( $\Delta\Delta\lambda\lambda$ ), or heterochiral  $C_3$  ( $\Delta\Delta\Delta\lambda / \lambda\lambda\lambda\Delta$ ) point symmetry and it significantly depends on the rigidity and nature of the substituted diaminoterphenyl precursor, for instance, 2,2''-dimethylterphenylenediamine (**A8**) afforded  $T$ -symmetry diastereomer, 2',5'-dimethylterphenylenediamine (**A10**) produced  $C_3$ -symmetric cage to a greater degree whereas, 2',3',5',6'-tetramethylterphenylenediamine (**A9**) predominantly generated  $S_4$  diastereomer cage (Figure 8). The substituents on diaminoterphenyl subcomponent not only influence the percentage of distribution of diastereomers at a particular temperature but to a certain extent influences the catalytic behaviour. For example, diaminoterphenyl subcomponent bearing chiral glyceryl group (**A20**) self-assembled with 2-formylpyridine (**C1**) and  $\text{FeSO}_4$  to form water soluble  $T$ -symmetric tetrahedral cage with a  $\text{Fe}^{\text{II}}-\text{Fe}^{\text{II}}$  distance and cavity volume of 17.1 Å and 418 Å<sup>3</sup> respectively. The glyceryl hydroxyl groups were hanging outwards from the hydrophobic cavity. The  $T$ -symmetric cage binds with a whole range of guests such as 1,3,5-triisopropylbenzene, limonene, camphor, *etc.*<sup>115</sup> and catalyzed the hydrolysis of pesticide and chemical warfare agents (CWA) simulant dichlorvos, generating dimethyl phosphoric acid (DMP) and dichlorovinylmethyl phosphoric acid (DVMP) as major and minor product respectively.<sup>115</sup>

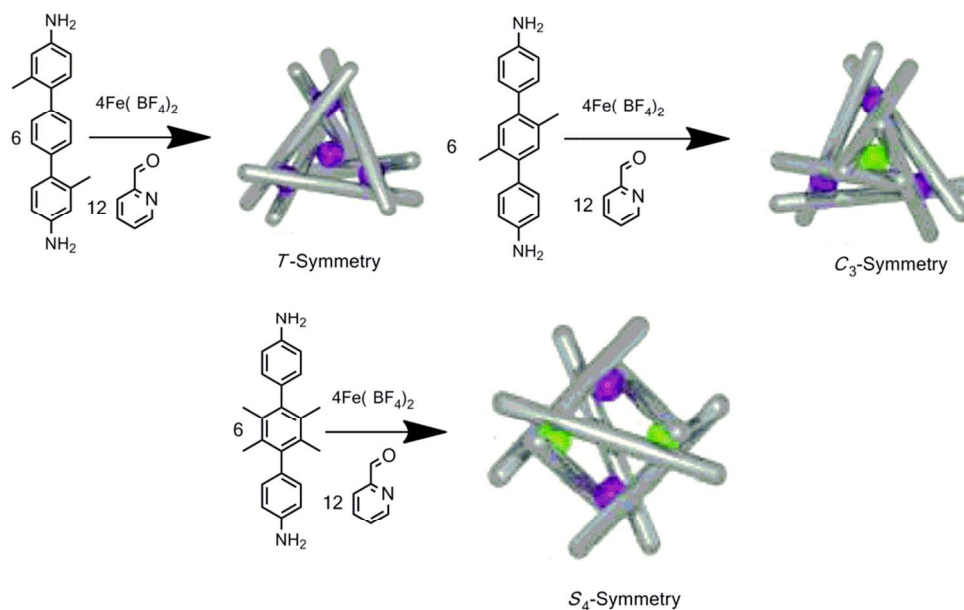


Figure 8 Three diastereomers of a tetrahedral  $M_4L_6$  capsule. Reprinted with permission from ref. 114 (Copyright © 2011 American chemical Society)

Apart from edge-directed tetrahedral, face-capped tetrahedral were also synthesized by imine linkers depending on the symmetry elements present in it.  $C_3$ -symmetric triamines with different spacer groups (**A11-A14**) generated azomethine linkage with 2-formyl pyridine (**C1**) and reacted with iron(II) in an appropriate stoichiometry to form  $T$ -symmetric face-capped  $[Fe_4L_4]^{8+}$  tetrahedra as shown in figure 9.<sup>116</sup> Due to the planar geometry of trianilines **A11**, **A13**, and **A14**, an alternative stoichiometry of 6 : 3 : 2 for aldehyde : triamine : iron(II) gave  $D_3$ -symmetric  $Fe_2L_3$  helicates. Among all, phenyl centered cage derived from **A13** in presence of template (cyclohexane) exhibited guest binding properties under the shadow of the size complementarity between the host cavity and guest and follows the binding strength order:  $CCl_4 > \text{cyclohexene} > \text{cyclopentane} > \text{cyclohexane} > \text{pyridine} > \text{cyclopentene} > \text{cyclohexanol} > \text{benzene} \gg \text{isoxazole, } CH_2Cl_2, CHCl_3 \text{ and } 1\text{-methylcyclopentanol}$ . Fascinatingly,  $n$ -pentane, higher  $n$ -alkanes up to  $n$ -octane did not bind with the cage as the entropic penalty that would be incurred during binding must give up several degrees of freedom in order to coil up into a compact structure.

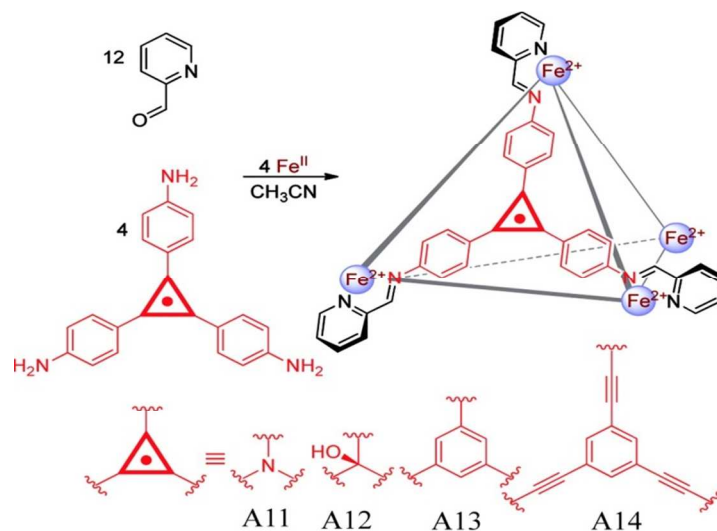
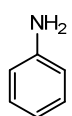
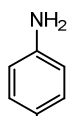
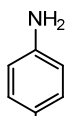


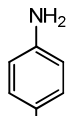
Figure 9: Subcomponent self-assembly of  $M_4L_4$  tetrahedral cage: Triamines **A11-A14**, 2-formylpyridine and iron (II) salts. Reprinted with permission from ref. 116 (Copyright © 2011 American Chemical Society).



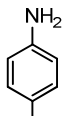
A1

X=Cl, Br, I  
A2

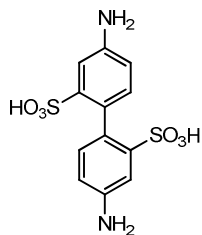
A3



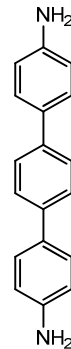
A4



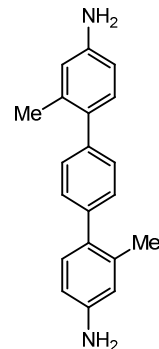
A5



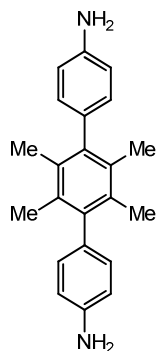
A6



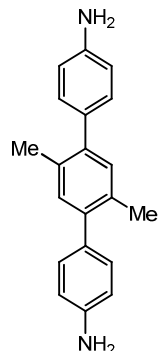
A7



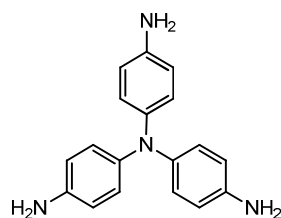
A8



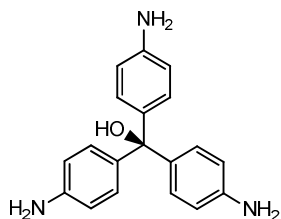
A9



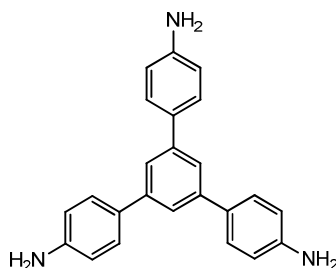
A10



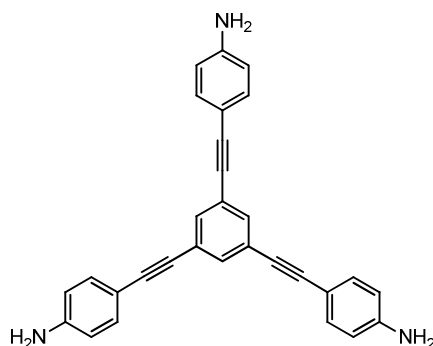
A11



A12



A13



A14



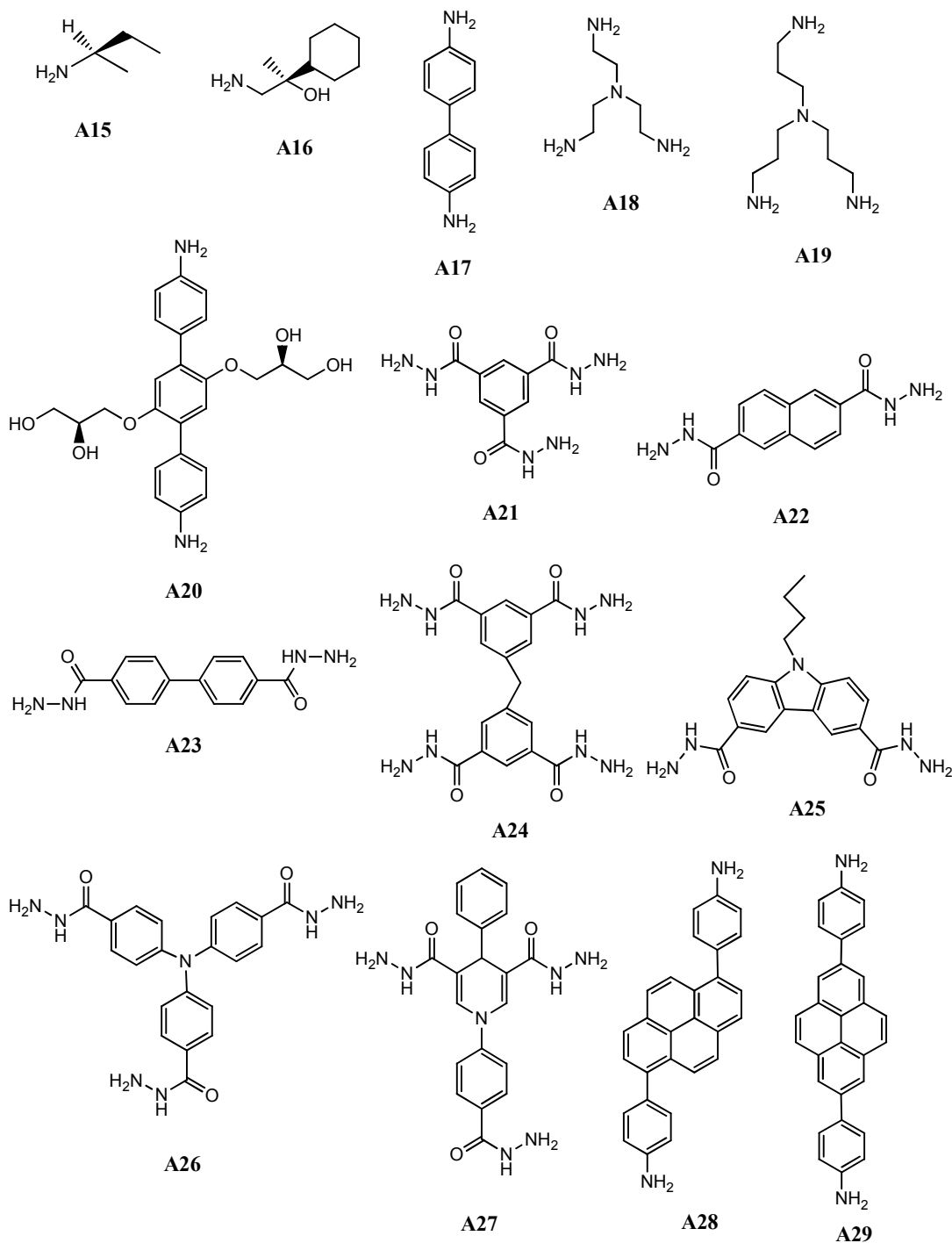


Figure 10. List of amines and substituted amines (A1-A29).

The geometry of polyhedra is dependent on the rigidity, spacer group between the binding moieties of subcomponents, template effect, and nature of solvent. An imine-linked M<sub>4</sub>L<sub>4</sub> tetrahedral was made from zinc metal ions and imine linker prepared by condensation of 2-

formylpyridine and  $C_3$ -symmetric tris(4-aminophenyl)methanol (**A12**) or 1,3,5-tri(4-aminophenyl)amine (**A13**) whereas, condensation of  $C_2$ -symmetric 4,4'-diaminobiphenyl (**A17**) afforded  $M_4L_6$  tetrahedra.<sup>117</sup> Both  $Zn_4L_4$  and  $Zn_4L_6$  cages underwent complete dismantling by addition of 4-methoxyaniline (**A4**) however, addition of 4 equivalents of 4-methoxyaniline to the mixture of  $Zn_4L_4$  and  $Zn_4L_6$  cages led to total disassembly of  $Zn_4L_4$  clearly implying the lower stability in comparison with the  $Zn_4L_6$  tetrahedral cage. This difference is explained by the slight strain within the framework.<sup>117</sup> Subcomponent self-assembly of linear 3,3'-bipyridine-6,6'-dicarboxaldehyde (**C8**) and aniline (**A1**) in the presence of an appropriate iron(II) salt led to the formation of  $T$ -symmetric  $[Fe^{II}_4L_6]^{8+}$  tetrahedral cage where, octahedral metal ions are at the vertex and  $C_2$ -symmetric bisbidentate pyridylimine ligand spanning at the edges<sup>118</sup>. Furthermore, the reaction of substituted amine, *p*-chloroaniline (**A2**) in place of unsubstituted aniline generated an analogous tetrahedral cage having *p*-chloroaniline at the exterior. The exterior of cage could be easily modified under the outline of electronic effects, as electron-poor aniline could be easily replaced by electron-rich-aniline. The reaction of substituted cage with *p*-toluidine (**A3**) or *p*-methoxyaniline (**A4**) led to the quantitative displacement of *p*-chloroaniline residues to the *p*-toluidine-containing and *p*-methoxyaniline-containing cage respectively. Moreover, the iron(II)-templated reaction of 3,3'-bipyridine-6,6'-dicarboxaldehyde (**C8**) with a mixture of *p*-bromoaniline, *p*-chloroaniline, and *p*-iodoaniline (**A2**) afforded a bunch of products (91 possible cages) but, addition of electron rich *p*-methoxyaniline led to the collapse of all possible cages and generated a *p*-methoxy substituted cage (Figure 11).<sup>118</sup>

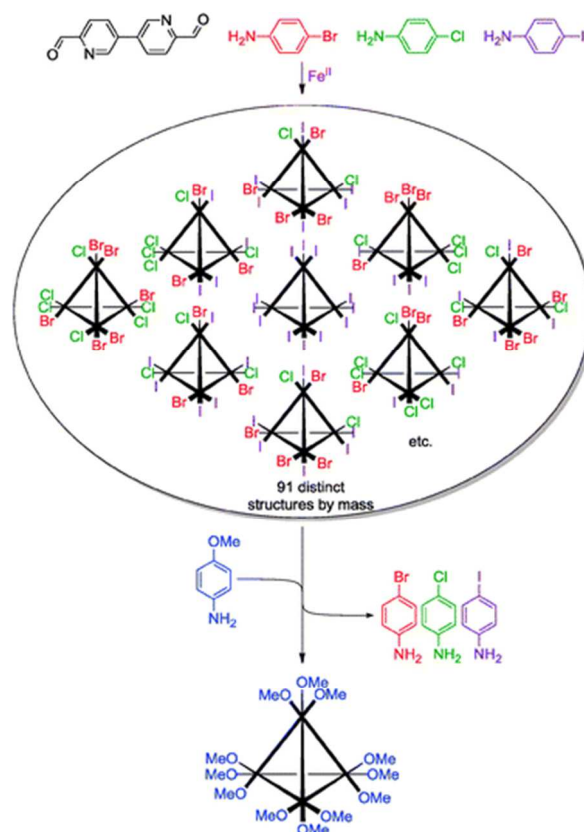


Figure 11. A library of heteroleptic tetrahedral cages and its transformation to a single homoleptic cage upon aniline substitution. Reproduced from ref. 118. (Copyright © The Royal Society of Chemistry)

Azomethine moiety formed by 5,5'-(1,4-phenylene)bis-2-pyridinecarboxaldehyde (**C10**) and anisidine (**A4**) self-assembled with iron(II) to form  $[\text{Fe}_4\text{L}_6]^{8+}$  tetrahedral cage. The  $C_2$ -symmetric bisbidentate pyridylimine ligands formed the edges of the tetrahedron, bridged between the four six-coordinated iron(II) ions at the vertices. The cage encapsulated a range of large sized anionic guests such as  $\text{BF}_4^-$ ,  $\text{PF}_6^-$ ,  $\text{NTf}_2^-$ ,  $\text{OTf}^-$ , and  $\text{ClO}_4^-$ .<sup>119</sup> Zinc(II)-templated helicate was synthesized from 3,3'-bipyridine-6,6'-dicarboxaldehyde (**C8**), tris(2-aminoethyl)amine (**A18**), and zinc trifluoromethanesulfonimide  $\text{Zn}(\text{NTf}_2)_2$  in acetonitrile and reduced to demetallated helicate by using sodium borohydride whereas, self-assembly of 3,3'-bipyridine-6,6'-dicarboxaldehyde (**C8**), tris(3-aminopropyl)amine (**A19**), and large sized Cd(II) ions afforded a tetrahedron (Figure 12).<sup>120</sup> The coordination of the central nitrogen atom of amine (**A19**) to the Cd(II) center appeared to spread the precursor in such a way as to favour the tetrahedral framework rather than  $\text{M}_2\text{L}_3$  helicates. Cadmium tetrahedron has a larger cavity volume as compared to helicate hence, effectively interacted with a range of guest molecules.

These guest molecules under the limelight of charge, non-covalent interactions, molecular shape, and aromaticity could be classified into various categories, Firstly, uncharged molecules such as phenanthrene, cyclooctane, cyclopentane, and hydrophilic or amphiphilic anions without aromatic groups (*e.g.* phosphate, nucleotide, or hexane-1-sulfonate) did not interacted at all secondly, hexafluorophosphate, aromatic mono- and dianions interacted with the cage and are in fast exchange between cavity and bulk solution on the NMR time scale.<sup>12</sup>

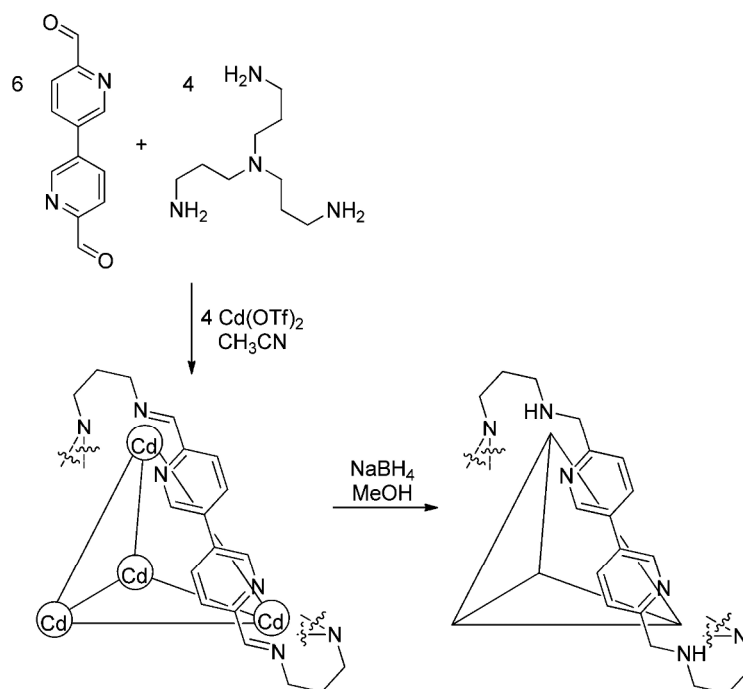


Figure 12. Synthesis of tetrahedra by reduction of the corresponding metal-organic precursors. Adapted from ref. 120 (Copyright ©2014 Wiley-VCH Verlag GmbH & Co. KGaA, Weinheim).

Not only achiral amines, chiral amines are also involved in synthesizing enantiopure cages *via* dynamic imine linkage and N→M coordination bond. The construction of well-defined larger chiral inner space is really a daunting task as change in precursor units precisely increment in length led to the framework of multiple stereochemical configurations. Fe<sub>4</sub>L<sub>6</sub> cage was synthesized by subcomponent self-assembly of linear 5,5'-bis(2-formylpyridines) with varying length of oligo-*p*-xylene spacers (**C9**) and chiral amines such as (*S*)-2-aminobutane (**A15**) and (*R*)-phenylglycinol. (**A16**).<sup>121</sup> The more bulky (*R*)-phenylglycinol generated cages with Fe<sup>II</sup> center and had a pronounced steric and  $\pi$ -stacking effect between phenyl and pyridyl rings albeit, less bulky (*S*)-2-aminobutane had a less effect upon the stereochemistry of Fe<sup>II</sup> stereocenters. The reaction of ligand with only one *p*-xylene spacer ( $n=1$ ) (**C9**) and (*R*)-phenylglycinol (**A16**)

afforded  $\text{Fe}_2\text{L}_3$  helicate and  $\text{Fe}_4\text{L}_6$  cage due to delicate balance in steric factors whereas, (*S*)-2-aminobutane (**A15**) formed only  $\text{Fe}_4\text{L}_6$  cage.<sup>121</sup> The larger cage derived from  $n=2$  or 3 had less stereochemical coupling between metal centers and entirely relies on the geometry and rigidity of the linkers.

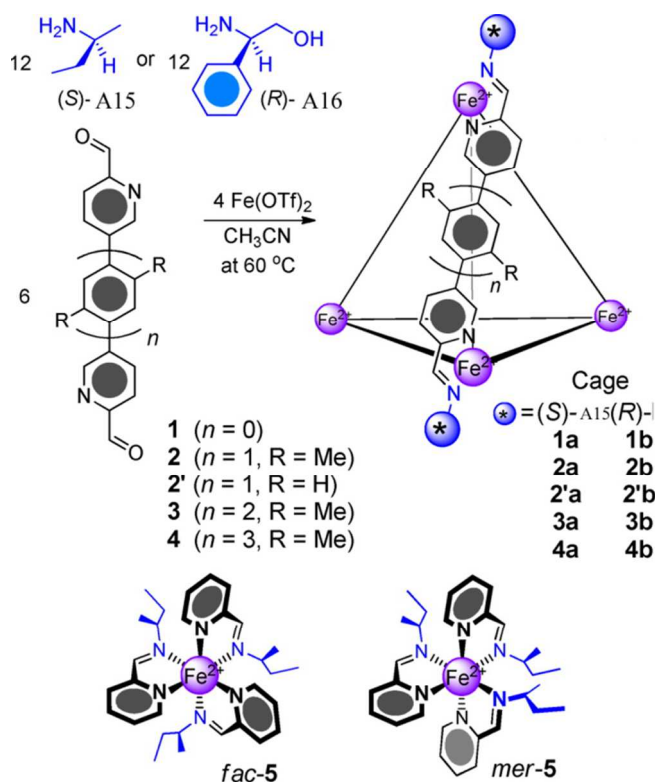


Figure 13. Diastereoselective formation of tetrahedral  $\text{Fe}_4\text{L}_6$  cage cages 1a-4a with less bulky chiral amine **A15** and 1b-4b with bulky chiral amine **A16**. Reprinted with permission from ref. 121 (Copyright © 2012 American Chemical Society)

Molecular recognition properties of the self-assembled cage based on self-assembly of iron (II) with amine-containing subcomponent and 2-formyl pyridine has been extraordinary.<sup>122,</sup>  
<sup>123</sup> 1,6-pyrene and 2,7-pyrene edged tetrahedral  $\text{Fe}_4\text{L}_6$  cages were recently synthesized by reaction of  $\text{Fe}(\text{NTf}_2)_2$ , 2-formyl pyridine (**C1**) and corresponding amine (**A28** or **A29**) in acetonitrile (Figure 14).<sup>124</sup> The percentage distribution of 1,6-pyrene tetrahedral cage consisted of 13% *T*, 42%  $C_3$ , and 45%  $S_4$  whereas, 2,7-pyrene edged tetrahedral cage comprised of 12% *T*, 45%  $C_3$ , and 43%  $S_4$ . The latter,  $\text{Fe}_4\text{L}_6$  cage has six ligands bridging the four octahedral iron (II) centers, three ligands displayed a *syn* conformation and other three adopts an *anti* conformation linking iron (II) centers. The metal-metal separations were in the range of 20.4-20.7 Å and 20.8-

20.9 Å for the *syn* and *anti* ligands respectively. 1,6-pyrene tetrahedral cage encapsulates a range of guests, categorizes into three classes, firstly, larger guests such as C<sub>60</sub>, C<sub>70</sub>, and coronene shows slow-exchange binding; secondly, guests such perylene, pyrene, triphenylene, diadamantane *etc.* are in fast-exchange binding; thirdly, tetracene, triptycene, and 1,4,5,8-naphthalene tetracarboxylic dianhydride were not encapsulated. On the other hand, 2,7-pyrene Fe<sub>4</sub>L<sub>6</sub> cage does not show any encapsulation behaviour.

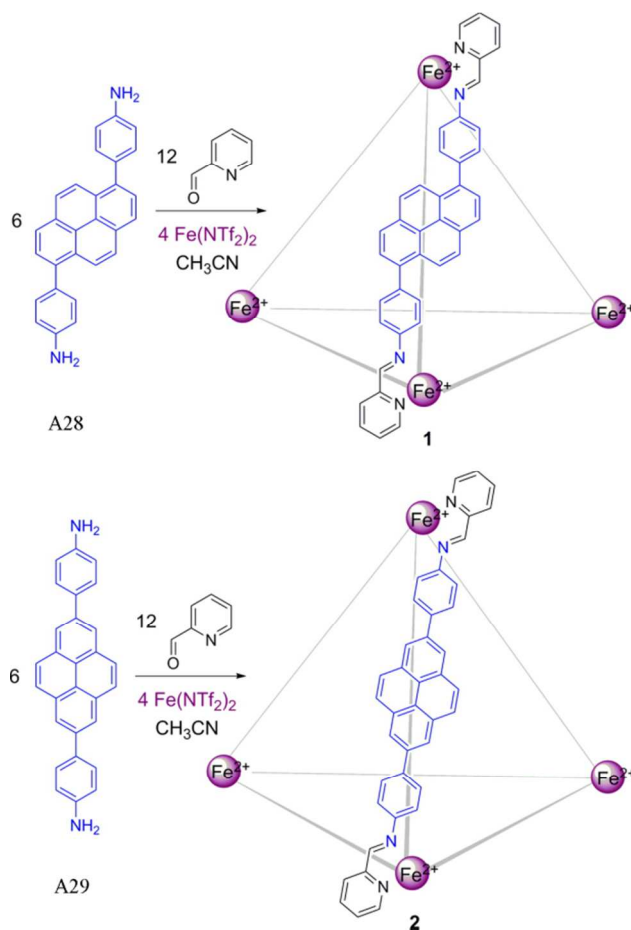


Figure 14. Preparation of [Fe<sub>4</sub>L<sub>6</sub>]<sup>8+</sup> tetrahedra **1** and **2** via subcomponent self-assembly of **C1** and **A28** or **A29**. Reprinted with permission from ref. 124 (Copyright © 2014 American Chemical Society)

Werner type tetrahedrons were synthesized by the self-assembly of cerium ions and imine linkers prepared by the condensation reaction of salicylaldehyde (**C4**) and 2,6-dicarbohydrazide naphthalene (**A22**) or 1,1'-dicarbohydrazide-4,4'-biphenyl (**A23**).<sup>125</sup> These M<sub>4</sub>L<sub>6</sub> tetrahedrons are composed of four vertical metal centers, each coordinated to three tridentate chelating groups in a coronary triangular prism coordination geometry whereas, each ligand positioned on one of the

six edges of the tetrahedron is defined by four metal ions and two bridged metal centers. Werner type tetrahedrons showed selective recognition of hexoses over smaller pentose and larger disaccharides. In addition to this,  $C_3$ -symmetric  $H_6TTS$  ( $N',N'',N'''$ -nitritotris-4,4',4''-(2-hydroxybenzylidene)-benzohydrazide) Schiff-base ligand prepared from the condensation reaction of 4,4',4''-nitritotribenzocarbonylhydrazide (**A26**) with salicylaldehyde (**C4**) is of utmost importance.<sup>126</sup> Self-assembly of amide containing tridentate chelated  $H_6TTS$  ligand with  $Ce^{III}$  ions generated  $Ce_4(H_2TTS)_4$  tetrahedron comprised of four vertical metal centers and four deprotonated  $H_2TTS$  ligands (Figure 15). Each cerium ions chelated by three tridentate chelating groups from three different ligands form a ternate coronary trigonal prism coordination geometry with a pseudo- $C_3$  symmetry. The metal ions separation and inner volume of the discrete tetrahedron was  $\sim 14.9 \text{ \AA}$  and  $360 \text{ \AA}^3$  respectively. The area of rhombic window was sufficient enough for ingress and egress of small guest molecules. This particular cerium tetrahedron is unprecedented on three important grounds firstly, it prompted the cyanosilylation of aldehydes with excellent selectivity as per substrate sizes<sup>127</sup> secondly, it effectively trapped nitric oxide over other mono anions<sup>126</sup> and thirdly in the detection of free tryptophan in serum.<sup>128</sup>

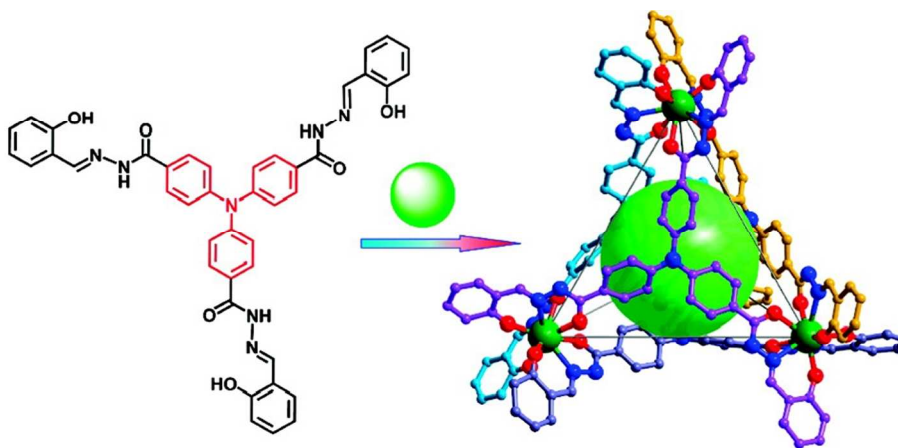


Figure 15. Structure of  $H_6TTS$  constitutive/constructional fragments of the functional tetrahedron. Reprinted with permission from ref. 126 (Copyright © 2011 American Chemical Society).

Salicylaldehyde is one of the important aldehydes employed in the construction of azomethine moieties, it reacted with 9-butyl-3,6-dicarbohydrazidecarbazole (**A25**) and 1-(4-(hydrazinecarbonyl)phenyl)-4-phenyl-1,4-dihydropyridine-5-dicarbohydrazide (**A27**) in methanol to form  $H_4ZL$  and  $H_6ZPS$  ligands, which on reaction with  $Ce(III)$  ions formed a basket-

like Ce-ZL metal-organic tetragon<sup>129</sup> and  $Ce_4(H_2ZPS)_4$  tetrahedron (Figure 16).<sup>130</sup> The structural constraints *i.e.* metal ions distance and inner cavity volume of the tetragon allowed incoming and outgoing of guests and encapsulated [FeFe]-H<sub>2</sub>ases to form hydrogen in the presence of sacrificial donor ( $N^iPr_2EtH.OAc$ ). Whereas,  $Ce_4(H_2ZPS)_4$  tetrahedron was used in selective sensing of most powerful explosive cyclo-trimethylene trinitramine (RDX) over trinitro toluene (TNT), dinitro toluene (DNT), *etc.*

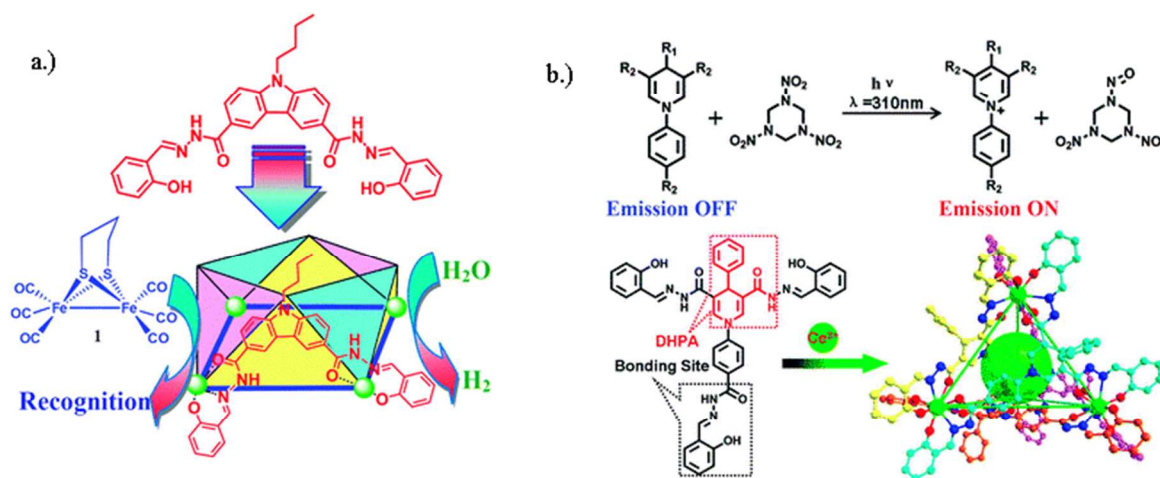


Figure 16. (a) Photoactive basket-like metal-organic tetragon, green ball represents the cerium ions. Reproduced from ref. 129. (b) The constitute/constructional fragments of Ce-ZPS. The metal, oxygen, and nitrogen are drawn in green, red, and blue respectively. Reproduced from ref. 130(Copyright © The Royal Society of Chemistry)

### 3.2 Octahedral and Cubic Imine Metal-organic polyhedra

Formation of supramolecular octahedral and cubic imine architectures is quite sporadic in the literature. Both assemblies have been achieved through edge- and face-directed self-assembly paradigms. In the former, the precursor sub units defines the edges of the cube whereas, in the latter the faces of the target assemblies are spanned by the imine linkers.

Duan *et al.* synthesized  $C_3$  and  $C_{2v}$  symmetric NATB and TBMS chelators by the condensation of 2-hydroxy-1-naphthaldehyde (**C6**) with 1,3,5-benzenetricarbohydrazide (**A21**) and 3,3',5,5'-tetracarbohydrazidediphenylmethane (**A24**) respectively. These chelator units self-assembled with cerium ions to form well-defined *T*-symmetric  $Ce_4(NATB)_4$  tetrahedron and  $Ce_8(TBMS)_6$  cube.<sup>131</sup>  $Ce_8(TBMS)_6$  cube is composed of eight metal ions and six TBMS chelators, all the cerium ions were positioned at the eight corners of the cube-like cage and were also nine-coordinated (Figure 17). The dihedral angle between two phenyl rings and the connected methylene group ranges from 55° to 60°. Generally, the coordination vector of the



imine ligands actually directed the construction of a particular class of polyhedra.  $M_4L_6$  tetrahedral cage was prepared by the self-assembly of rigid 4,4'-diimino-3,3'-bipyridine and octahedral  $Fe^{II}$  templates. The parallel orientation of the coordinate vectors with a bipyridine backbone directed the rational designing of  $M_nL_{3n/2}$  complex.<sup>64</sup> Edge-bridged  $M_8L_{12}$  cube on the other hand, prepared by the incorporation of ditopic 3,3'-diimino-4,4'-bipyridine having a coordination vectors into an obtuse orientation of less than  $120^\circ$ .<sup>132</sup> Mixing of iron(II) triflimide with dialdehyde (**C7**) and *p*-toluidine (**A3**) in acetonitrile formed a *T*-symmetric cationic  $[Fe_8L_{12}]^{16+}$  capsule having an average metal-metal distance of 11 Å and internal volume of 1000 Å<sup>3</sup> whereas, incorporation of 4-decylaniline (**A5**) afforded a similar cage with alkyl part hanging outside to it.<sup>133</sup> The former interacted with ferrocene over decamethylferrocene and acetylferrocene in MeCN whereas, the latter showed interaction with 9-acetylanthracene in preference to anthracene, pyrene, and 1-acetylpyrene under the shadow of noncovalent interactions such as coulombic, dipole-dipole,  $\pi$ - $\pi$  quadrupolar interactions.

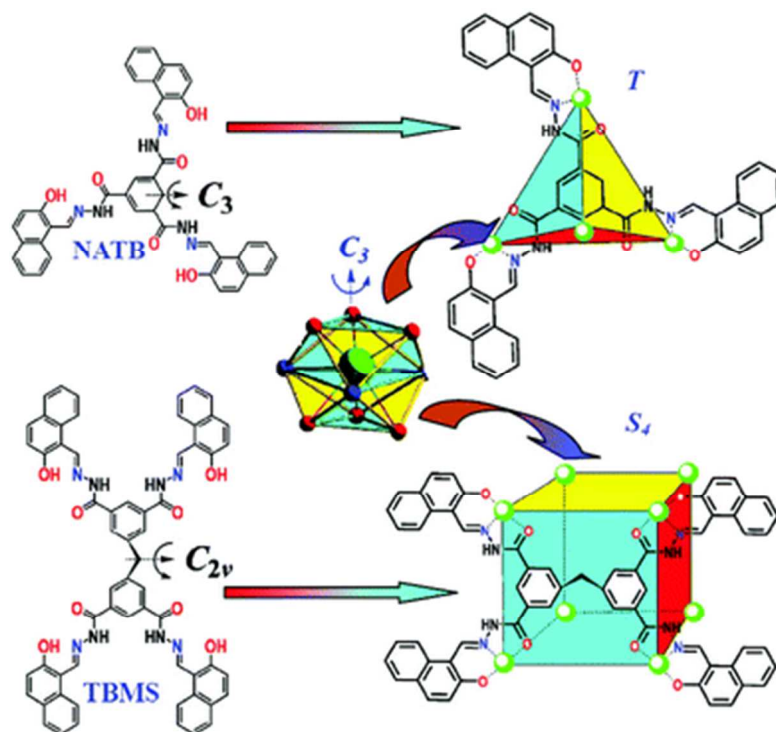


Figure 17. A schematic representation of the generation of the polyhedra by well-positioned cerium centers and the ligands having tridentate NOO chelators. Reproduced from ref. 131 (Copyright © The royal society of Chemistry)

The stable azomethine moiety can also be constructed by the condensation reaction of carbonyl compounds and mono substituted ammonia derivatives such as  $\text{NH}_2\text{-G}$  where  $\text{-G}$  has a  $\text{-I}$  or  $\text{-M}$  effect like  $\text{-OH}$ ,  $\text{-NH}_2$ , *etc.* A  $C_3$ -symmetric facial ligand with  $\text{N}_2\text{O}$  tridentate chelator was synthesized by the Schiff-base reaction of 2-quinolinecarboxaldehyde (**C5**) and 1,3,5-benzenetricarbohydrazide (**A21**) in ethanol. Self-assembly of this disk-shape linker with  $\text{Co}^{\text{II}}$  or  $\text{Zn}^{\text{II}}$  perchlorate led to the formation of Cobalt or Zinc octahedral nanocages.<sup>134</sup> These octahedral cationic cages have an ideal  $C_3$  and pseudo  $S_4$  symmetry achieved by alternative arrangement of the four planar ligands onto the eight triangular faces of the octahedron defined by six metal ions. Using pyridine instead of quinoline moieties afforded a similar  $C_3$ -symmetric disk-shaped ligand with retention of the  $\text{N}_2\text{O}$  tridentate units afforded  $\text{Ni}^{\text{II}}$ ,  $\text{Eu}^{\text{III}}$ , and  $\text{Tb}^{\text{III}}$  octahedral cages (Figure 18). Furthermore, the presence of amide functionalities within the positively charged cages imparted static, geometric, coordinative, and functional properties required for the recognition of ribonucleosides,<sup>135</sup> monosaccharide derivatives such as glucosamine.<sup>136-138</sup>

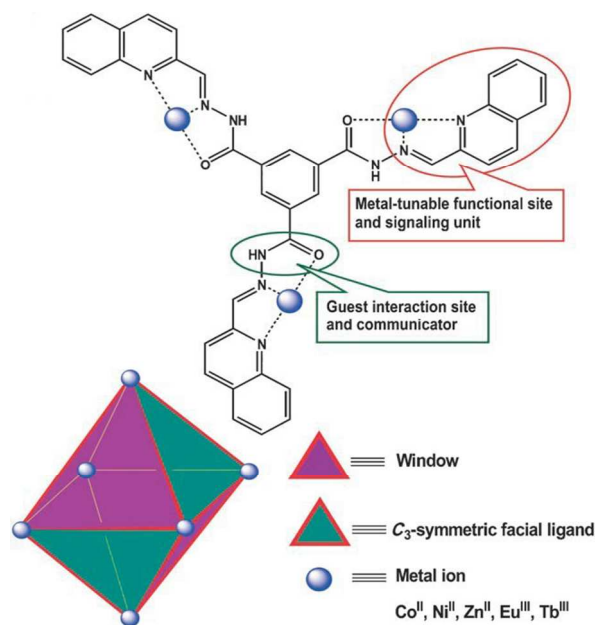


Figure 18. Structure of quinolone derivative ligand and constitutive/constructional fragments of the functional octahedral cages. Adapted from ref. 134 (Copyright © 2008 Wiley-VCH Verlag GmbH & Co. KGaA, Weinheim).

Nitschke's group recently reported the subcomponent self-assembly of a large and complex cubic structure incorporating two different metal ions  $\text{Fe}^{\text{II}}$  and  $\text{Pt}^{\text{II}}$  /  $\text{Pd}^{\text{II}}$ .<sup>139</sup> Moreover,

self-assembly of 2-formylpyridine, *cis*-bis(benzonitrile)dichloroplatinum(II), silver triflate, and cadmium(II) trifluoromethanesulfonate in acetonitrile at 50°C for 8 h affords a  $M_8L_6$  cube (Figure 19).<sup>140</sup> The eight tris(pyridylimine)cadmium vertices in the cage have facial stereochemistry with  $C_s$  point symmetry and is energetically favourable due to C-H $\cdots\pi$  interactions between neighbouring anthracenes around the corner. The diagonal distance across the cube from the outermost hydrogen atoms of the farthest-spaced ligands is 5.0 nm.  $M_8L_6$  cage encloses a cavity of 4225 Å<sup>3</sup>, which dynamic motion in solution might further increases to up to 7000 Å<sup>3</sup>. Neutral guests were unable to be encapsulated inside the cavity however, anionic species such hexamolybdate ( $Mo_6O_{19}^{2-}$ ), dodecafluoro-*closo*-dodecaborate ( $B_{12}F_{12}^{2-}$ ), tetraphenylborate ( $BPh_4^-$ ), carborane ( $CB_{11}H_{12}^-$ ), and tetrakis(pentafluorophenyl)borate ( $B(C_6F_5)_4^-$ ) effectively bind with the cage. Dianions ( $Mo_6O_{19}^{2-}$  and  $B_{12}F_{12}^{2-}$ ) bind more strongly than the monoanions ( $BPh_4^-$ ,  $CB_{11}H_{12}^-$ ,  $B(C_6F_5)_4^-$ ) under the shadow of electrostatic force of attraction and larger anions favoured over smaller ones.<sup>140</sup>

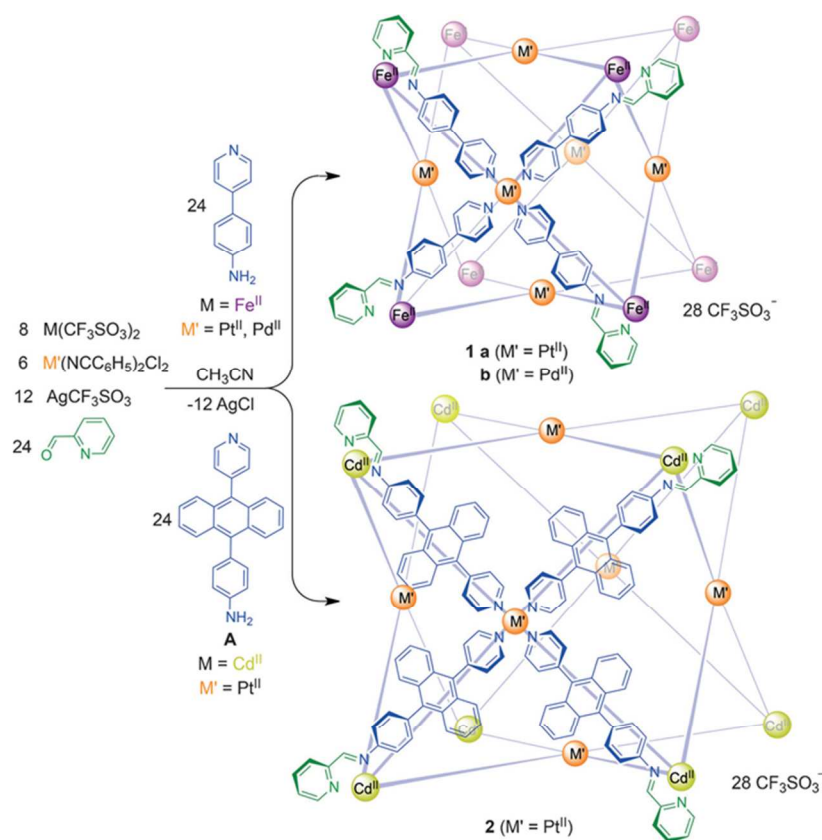


Figure 19. The one-pot procedure for cube 1a, 1b, and 2 from subcomponents and metal ions, only one cube face is shown for clarity. Adapted from ref. 140 (Copyright © 2015 Wiley-VCH Verlag GmbH & Co. KGaA, Weinheim).

Cu(I) can preferentially form heteroleptic complexes containing two phosphine and two nitrogen donors due to steric factors<sup>141</sup>. For instance, reaction of Cu(I) with linear 1,4-bis(diphenylphosphino)benzene (**B**) and 2,2'-bipyridine affords  $[(2,2'\text{-bipy})\text{Cu}^{\text{I}}]_2\text{B}_2$  whereas, tetrakis(4-iminopyridyl)porphyrinatozinc(II) ligand (**A**) in place of 2,2-bipyridine led to  $[\text{Cu}^{\text{I}}_8\text{A}_2(\text{diphosphine})_8]$ . The same group recently reported the synthesis of prism **1** as bis(quinuclidine) host-guest complex  $[\text{Q}_2\text{c}1]$  by sub component self-assembly of 5,10,15,20-tetrakis(4-aminophenyl)porphyrinatozinc(II) (Zn-TAPP), diposphine **B**, 2-formylpyridine and tetrakis(acetonitrile)copper(I) bis(trifluoromethylsulfonyl)imide  $[\text{Cu}(\text{MeCN})_4]\text{NTf}_2$  in DMF (Figure 20).<sup>142</sup> Quinuclidine binds at an axial position to the porphyrinatozinc(II) subcomponent self-assembly, under the limelight of effective axial position binding, 3,3'-bipyridine selectively encapsulates through ditopic axial coordination to the zinc (II) subcomponent. Moreover, reaction of 4,4'-bipyridine responds in a similar fashion however, it preferred *exo* binding, while 2,2-bipyridine cannot bind to the prism due to the steric constraints. Prism **1** guest-binding efficiency depends on the coordination of porphyrin  $\text{Zn}^{\text{II}}$  centers,  $[(4,4'\text{-bipy})1]$  is selective for coordination guest, coordination ligand such as DABCO, triethylamine, quinolone, isoquinoline, and quinidine did not exhibit well-defined binding due to steric clashes with the host.

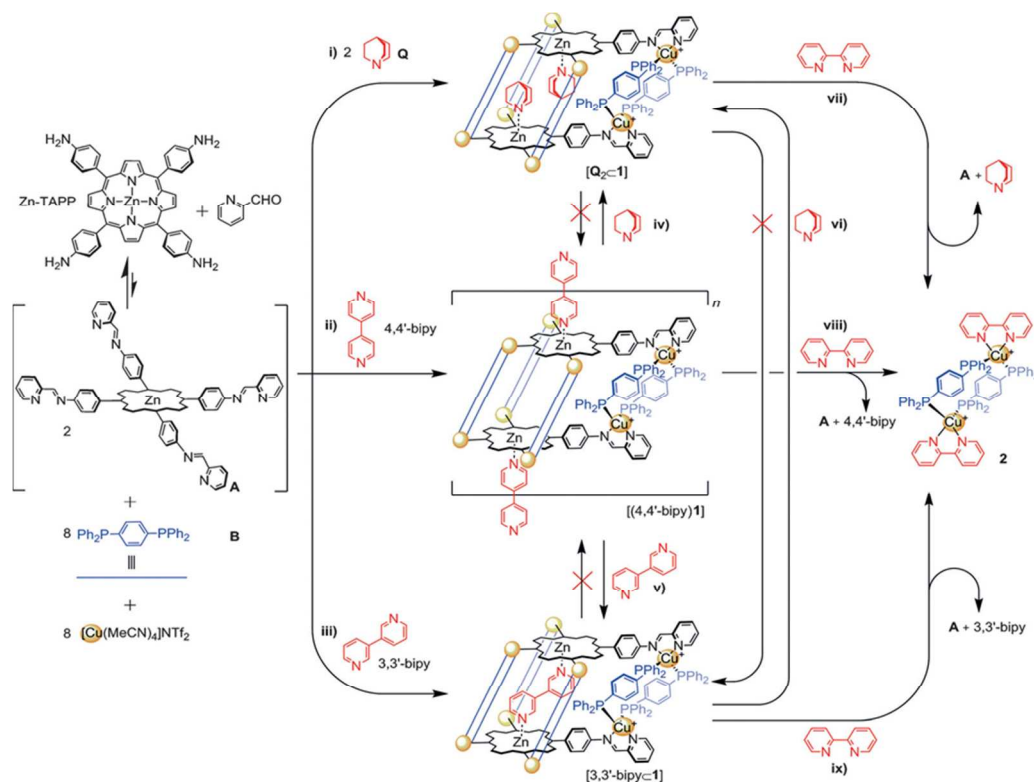


Figure 20. Self-assembly of  $C_4$ -symmetric tetrakis(bidentate) ligand **A**, **C1**, 1,4-bis(diphenylphosphino)benzene **B**, and  $[\text{Cu}(\text{MeCN})_4]\text{NTf}_2$  with quinuclidine (Q) and three bipyridine isomers (2,2', 3,3', and 4,4') in DMF to form prisms i)  $[\text{Q}_2\text{C}1]$  ii)  $[(4,4'\text{-bipy})\text{C}1]$  iii).  $[(3,3'\text{-bipy})\text{C}1]$ . Adapted from ref. 142 (Copyright © 2015 Wiley-VCH Verlag GmbH & Co. KGaA, Weinheim).

### 3.3 Icosahedral Imine Metal-organic polyhedra

Icosahedron is one of the polyhedron with 20 faces, rarely highlighted in the literature. Nitschke's group synthesized mixture of products *i.e.*  $\text{Fe}_2\text{L}_3$  helicates, tetrahedral capsule, and a small percentage of icosahedral framework by reaction of Iron (II), 2-formylpyridine (**C1**) and **A13** in the absence of template. The percentage yield of  $\text{Fe}^{\text{II}}_{12}\text{L}_{12}$  icosahedral framework (Figure 21) could be increased by using more polar solvents methanol:acetonitrile and also by increasing the concentration of metal ions from 25.4 mM to 46.5 mM.<sup>143</sup> The icosahedral framework preferred to bind only dodecafluoro-*closo*-dodecaborate  $[\text{B}_{12}\text{F}_{12}]^{2-}$  over neutral molecule of similar or larger size anions such as tetrakis(pentafluorophenyl)borate and tetraphenylborate under the sway of non-covalent interactions.

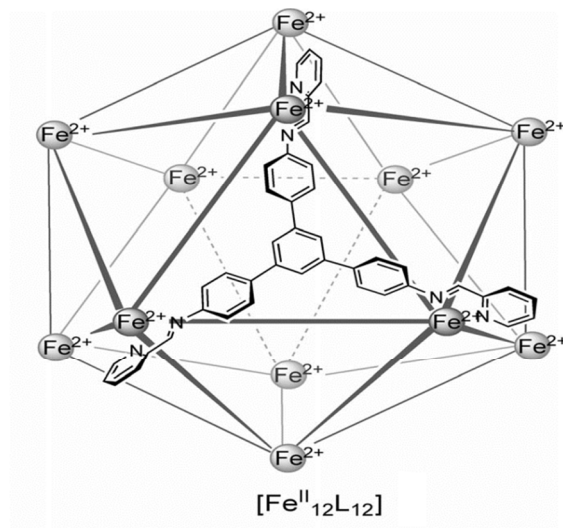


Figure 21. Self-assembled icosahedral framework preferred in 50:50 (v/v) methanol/acetonitrile solution at 343K. Adapted from ref. 143 (Copyright © 2013 Wiley-VCH Verlag GmbH & Co. KGaA, Weinheim)

Table 1: A tabulation of polyhedron geometry derived from aldehyde, amines, and metal ions.

S.No.	Aldehydes (C)	Amines (A)	Metal ions (M)	Geometry	Ref.
1	C1	A6	Fe(II), Co(II), Ni(II)	M <sub>4</sub> L <sub>6</sub> Tetrahedron	108, 112
2	C1	A8/A9/A10	Fe(II)	M <sub>4</sub> L <sub>6</sub> Tetrahedron	114
3	C1	A20	Fe(II)	M <sub>4</sub> L <sub>6</sub> Tetrahedron	115
4	C1	A11/A13/A14	Fe(II)	M <sub>2</sub> L <sub>3</sub> Helicate / M <sub>4</sub> L <sub>4</sub> Tetrahedron	116
5	C1	A12/A13	Zn(II)	M <sub>4</sub> L <sub>4</sub> Tetrahedron	117
6	C1	A17	Zn(II)	M <sub>4</sub> L <sub>6</sub> Tetrahedron	117
7	C8	A1/A2/A3/A4	Fe(II)	M <sub>4</sub> L <sub>6</sub> Tetrahedron	118
8	C10	A4	Fe(II)	M <sub>4</sub> L <sub>6</sub> Tetrahedron	119
9	C8	A18	Zn(II)	M <sub>2</sub> L <sub>3</sub> Helicate	120
10	C8	A19	Cd(II)	M <sub>4</sub> L <sub>6</sub> Tetrahedron	120
11	C7	A3/A5	Fe(II)	M <sub>8</sub> L <sub>12</sub> Cube	133
12	C5	A21	Co(II), Zn(II), Ni(II)	M <sub>6</sub> L <sub>4</sub> Octahedron	134
13	C4	A22/A23	Ce(III)	M <sub>4</sub> L <sub>6</sub> Tetrahedron	125
14	C6	A21/A24	Ce(III)	M <sub>4</sub> L <sub>4</sub> Tetrahedron/M <sub>8</sub> L <sub>6</sub> Cube	131
15	C4	A25/A26/A27	Ce(III)	M <sub>4</sub> L <sub>4</sub> tetrahedron	129, 126,130
16	C9	A15/A16	Fe(II)	M <sub>2</sub> L <sub>3</sub> Helicate/M <sub>4</sub> L <sub>6</sub> Tetrahedron	121
17	C1	A28/A29	Fe(II)	Tetrahedron	124

#### 4. Imine based frameworks

Dynamic imine chemistry has also been utilized in the construction of crystalline three dimensional molecular prisms<sup>144</sup> and organic adamantanoid.<sup>145</sup> Recently, Yaghi and co-workers

constructed permanent porous 3D framework materials containing C–N and C–C linkage. The solvothermal reaction of the rigid tetrahedral building block tetra-(4-anilyl)-methane with linear terephthaldehyde afforded covalent organic frameworks (COFs) with a diamond topology.<sup>146</sup> The framework has a high percentage of C=N bond resulted in great thermal stability up to 490°C and has demonstrated permanent porosity with a surface area of 1360 m<sup>2</sup>g<sup>-1</sup>. The same group also reported that when planar building blocks instead of tetrahedral building block were used, extended 2D porous frameworks could be formed for instance, 1,3,5-triformylbenzene or 1,3,5-tris(4-formylphenyl)benzene condensed with 2,5-diethoxyterephthalohydrazide to form thermally stable extended hydrazone linked covalent organic frameworks.<sup>147</sup> The structural restraints of COFs make them prominent candidates for catalysis, and were highlighted by Wang's group. An imine-linked porous 2D COF synthesized from 1,3,5-triformylbenzene and 1,4-diaminobenzene effectively incorporated Pd<sup>II</sup> ions through Schiff base ligand-metal coordination. The resulting stable Pd/COF displayed an excellent activity in catalyzing the Suzuki-Miyaura coupling reaction.<sup>148</sup> The unprecedented catalytic activity is due to the unique structure of Pd/COF, which provide efficient access to the catalytic sites.

Kanatidis and Nguyen's group synthesized an imine-linked microporous polymer organic framework (POF) from 1,3,5-triformylbenzene and 1,4-diaminobenzene or 1,3-diaminobenzene derivative.<sup>149</sup> The resulting framework exhibited high Brunauer-Emmett-Teller (BET) surface areas up to 1500 m<sup>2</sup>g<sup>-1</sup>, and a high isosteric heat of H<sub>2</sub> adsorption up to 8.2 KJ/mol. Due to surface functionality within the pore, the POFs are used in selective recognition and gas separation. The coordination ability of the imine moiety has been heavily utilized in the preparation of helicates and sandwich complexes for example, reaction between mono (phthalocyaninato) rare earth-metal complex and Schiff base ligands precisely, *N,N'*-bis(3-methoxysalicylidene)-benzene-1,2-diamine led to the unexpected sandwich-type quadruple-decker structure [CaM<sub>2</sub>(Pc)<sub>2</sub>(L)<sub>2</sub>(CH<sub>3</sub>OH)<sub>2</sub>] (M=Y, Dy).<sup>150</sup> Ca<sup>2+</sup> ions act as a mediator in connecting two phthalocyaninato-Schiff base rare-earth double-decker units into the quadruple-decker. Furthermore, H<sub>4</sub>DBDS, H<sub>4</sub>DBOS, and H<sub>4</sub>DBBS imine ligand self-assembled with Ce(III) ions to form Ce<sub>2</sub>(DBDS)<sub>3</sub>, Ce<sub>2</sub>(DBOS)<sub>3</sub>, and Ce<sub>2</sub>(DBBS)<sub>3</sub> helicates respectively.<sup>151</sup> These C<sub>3</sub>-symmetric molecular lanterns are comprised of three deprotonated ligands and two cerium metal ions. Each cerium ion was coordinated to three identical NOO tridentate chelators from three ligands in a ternate coronary trigonal prism geometry. The geometrical constraints of the internal

cavities provided high selectivities to the Ce-DBBS and Ce-DBDS lantern-type probes towards the  $\text{Mg}^{2+}$  ion over other alkali and alkaline metal ions whereas, Ce-DBOS was employed as an artificial chemosensor for selective detection of  $\text{Al}^{3+}$  in comparison to  $\text{Mg}^{2+}$  ions.

As explained above, the extension of dynamic covalent chemistry to covalent bond is interesting to reach new structures but might require the activation of the exchange process using catalysts. For instance, one example of such a catalyzed exchange was applied to poorly dynamic hydrazone units for the generation of libraries of helical strands.<sup>5, 6</sup> In this work, the enforced self-assembly of helical strands by formation of reversible hydrazone-type bonds between pyrimidine based helicity codons gives access to dynamic libraries of molecular helices. To activate the exchange process and general diversity, a  $\text{Sc}(\text{OTf})_3$  catalysis was first developed to generate isoenergetic libraries,<sup>4</sup> thus avoiding any kind of stabilization of a particular product of the library by the catalyst itself. For instance, figure 22 displays the chemical structure of a one turn helical strand **1**, being represented here as its linear form for the sake of clarity and containing four hydrazone groups. The date analysis demonstrated that full recombination between **1** and dihydrazine-pyrimidine takes place under activation by 4% catalyst. In these conditions, the library of compound **1-28** was obtained, containing expanded helices of up to 10 hydrazones sites (more than 3 helical turns). Moreover, all the possible cross combinations with phenyl and/or methoxyphenyl moieties were generated for each size of helical strand, highlighting the efficiency of reorganization process. Interestingly, the production of product **2** among the members of the library allows the subsequent full reorganization of such libraries, indeed, by adding  $\text{Zn}^{\text{II}}$  ions, two-site ligand **2** can self-assemble to yield grid-type complex  $\text{Zn}_4(\mathbf{2})_4$ .



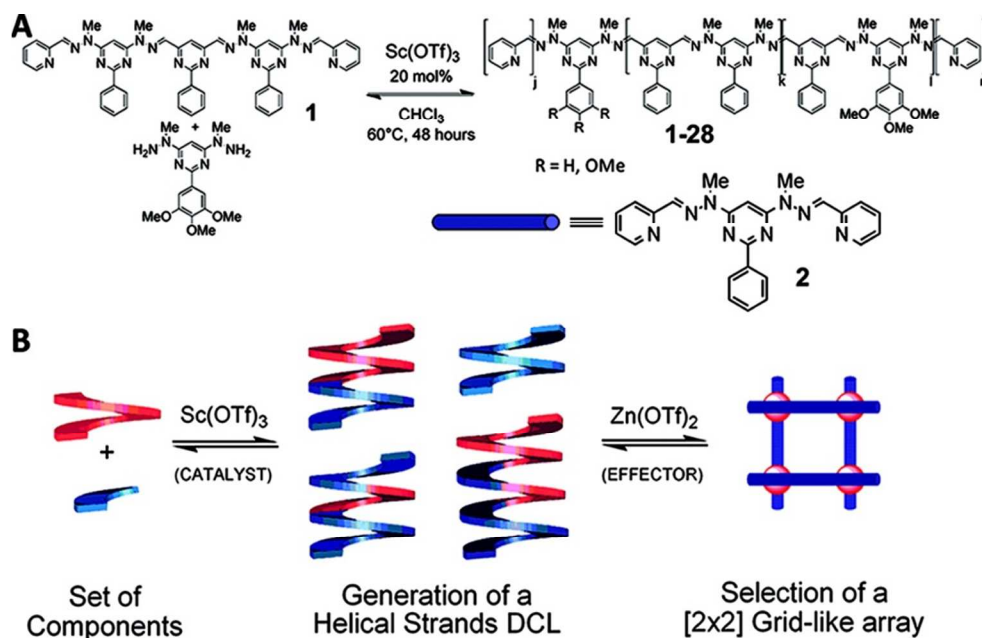


Figure 22. (A) Generation of a library of helices starting from one-turn/4 sites helical compound **1** and dihydrazinopyrimidine using  $\text{Sc}(\text{OTf})_3$  as catalyst. (B) Schematic representation of the system: (left) Lewis acid-catalyzed generation of dynamic constitutional diversity in helical molecular strands; (right)  $\text{Zn}^{\text{II}}$  recombination toward  $[2 \times 2]$  grid formation. Adapted from ref. 5 (Copyright © 2004 Wiley-VCH Verlag GmbH & Co. KGaA, Weinheim)

In 2013, Lehn and co-workers reported<sup>152</sup> the grid-double-helicate interconversion by reaction of a mixture of ligands **1** and **2** with  $\text{CuI}$  to form three binuclear double helicates, namely two homoleptic  $[\text{Cu}_2\mathbf{1}_2]^{2+}$  and  $[\text{Cu}_2\mathbf{2}_2]^{2+}$  and one heteroleptic  $[\text{Cu}_2(\mathbf{1})(\mathbf{2})]^{2+}$ . However, reaction of any one of the ligands with  $\text{Cu}(\text{CF}_3\text{SO}_3)_2$  produces tetranuclear  $[2 \times 2]$  grid-like complex  $[\text{Cu}_4\mathbf{1}_4]^{8+}$  or  $[\text{Cu}_4\mathbf{2}_4]^{8+}$ . Additionally, the double helicate  $[\text{Cu}_2\mathbf{1}_2]^{2+}$  conversion to grid  $[\text{Cu}_4\mathbf{1}_4]^{8+}$  operates to metal ions displacement:  $2[\text{Cu}_2\mathbf{1}_2]^{2+} + 4\text{Cu}_2^+ \rightarrow [\text{Cu}_4\mathbf{1}_4]^{8+} + 4\text{Cu}^+$  however, vice versa has been done by the treatment with four equivalent of  $\text{CF}_3\text{SO}_3\text{H}$ , then with 1-1.5 equiv. of ascorbic acid and at last treated with triethylamine. The interconversion between double helicates and mononuclear complexes,<sup>153, 154</sup> ring and cage molecule,<sup>155</sup> macrocycle and polymer,<sup>156</sup> grid- and pincer-like molecule,<sup>157</sup> assembled and disassembled state of 2D and 3D architectures,<sup>158</sup> as well as other type of interconversion<sup>159, 160</sup> are also well reported in the literature.

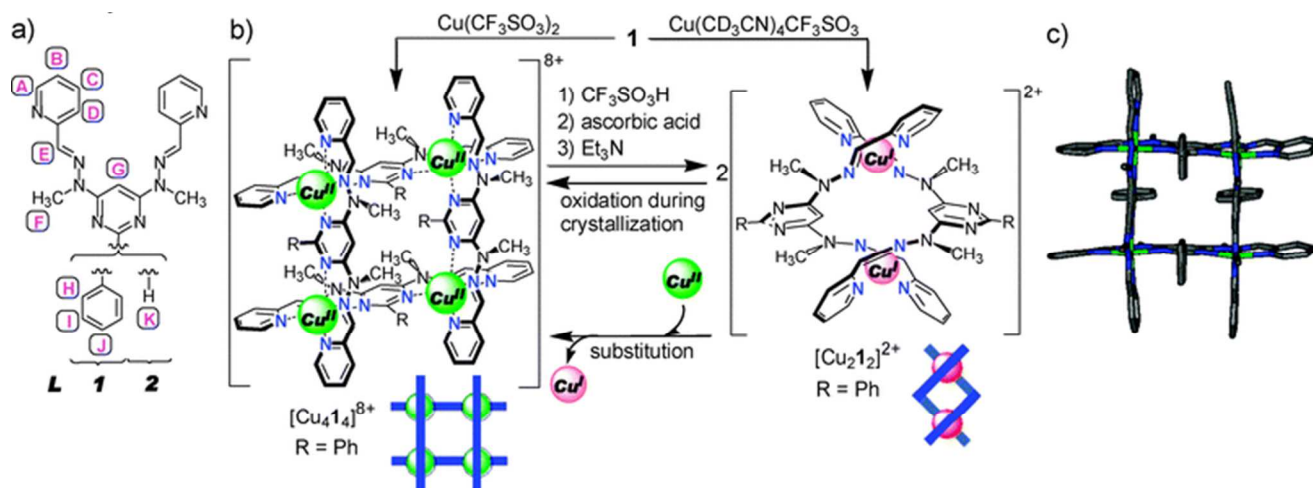


Figure 23. (a) Structural formulae of ligands **1** and **2**; (b) Scheme of the interconversion between grid  $[\text{Cu}_4\mathbf{1}_4]^{8+}$  and double helicates  $[\text{Cu}_2\mathbf{1}_2]^{2+}$ ; (c) X-ray molecular structure of grid  $[\text{Cu}_4\mathbf{1}_4]^{8+}$  (H atoms and anions were omitted for clarity) Reproduced from ref. 152 (Copyright © The royal society of Chemistry)

## 5. Conclusion

The centuries old imine chemistry offers an entirely new approach in the preparation of self-assembled architectures. Metal-organic polyhedra are three-dimensional discrete structures typically synthesized by the self-assembly of symmetrical imine linkers and metal ions. The range of carbonyl compound and amines or substituted amines employed in the preparation of imines has been tangibly elaborated and their incorporation in the construction of polyhedra of various geometries is further exaggerated under different headings. More importantly, the dynamic nature of imine bonds is partially or completely preserved in the final structure which in turn imparts robustness to it. This retention of imine moiety in the structures not only reveal differentiability from other polyhedra prepared by the self-assembly of metal ions with linkers having  $-\text{COOH}$  groups oriented in different bend angles or exo-/endo-functionized bis(pyridine) ligands, but also makes them suitable for encapsulations of various guest molecules of different size and shapes. The polarity and rich chemistry associated with amines, carbonyl compounds along with plethora of metal ions opens a permutation and combination for proper tuning of self-assembled architectures and these structures under the sway of new discoveries can hold a great promise for energy, environmental, and biological applications.

## Acknowledgments

The authors would like to express their deep accolade to “State Key Laboratory of Advanced Technology for Materials Synthesis and Processing” for financial support. F.V. acknowledges the Chinese Central Government for an “Expert of the state” position in the program of “Thousand talents” as well as the support of the National Science Foundation of China (No. 21172027). H.V and I.N express their deep appreciation to the Chinese Scholarship Council (CSC) for the financial support for their PhD study grant 2013GXZ989 and 2014GXZ328 respectively.

## References

1. H. Schiff, *Justus Liebigs Ann. Chem.*, 1864, **131**, 118-119.
2. S. J. Rowan, S. J. Cantrill, G. R. Cousins, J. K. Sanders and J. F. Stoddart, *Angew. Chem. Int. Ed.*, 2002, **41**, 898-952.
3. D. Schultz and J. R. Nitschke, *J. Am. Chem. Soc.*, 2006, **128**, 9887-9892.
4. N. Giuseppone, J.-L. Schmitt, E. Schwartz and J.-M. Lehn, *J. Am. Chem. Soc.*, 2005, **127**, 5528-5539.
5. N. Giuseppone, J.-L. Schmitt and J.-M. Lehn, *Angew. Chem. Int. Ed.*, 2004, **43**, 4902-4906.
6. N. Giuseppone, J.-L. Schmitt and J.-M. Lehn, *J. Am. Chem. Soc.*, 2006, **128**, 16748-16763.
7. M. Ciaccia, R. Cacciapaglia, P. Mencarelli, L. Mandolini and S. Di Stefano, *Chem. Sci.*, 2013, **4**, 2253-2261.
8. C. K. Ingold and H. A. Piggott, *J. Am. Chem. Soc.*, 1922, **121**, 2793-2804.
9. C. K. Ingold and H. A. Piggott, *J. Am. Chem. Soc.*, 1923, **123**, 2745-2752.
10. K. E. Meyer, P. J. Walsh and R. G. Bergman, *J. Am. Chem. Soc.*, 1994, **116**, 2669-2670.
11. K. E. Meyer, P. J. Walsh and R. G. Bergman, *J. Am. Chem. Soc.*, 1995, **117**, 974-985.
12. S. W. Krska, R. L. Zuckerman and R. G. Bergman, *J. Am. Chem. Soc.*, 1998, **120**, 11828-11829.
13. R. L. Zuckerman, S. W. Krska and R. G. Bergman, *J. Am. Chem. Soc.*, 2000, **122**, 751-761.
14. G. K. Cantrell and T. Y. Meyer, *J. Am. Chem. Soc.*, 1998, **120**, 8035-8042.

15. J. M. McInnes and P. Mountford, *Chem. Commun.*, 1998, 1669-1670.
16. M. C. Burland, T. W. Pontz and T. Y. Meyer, *Organometallics*, 2002, **21**, 1933-1941.
17. M. Ciaccia and S. D. Stefano, *Org. Biomol. Chem.*, 2015, **13**, 646-654.
18. Y. Jin, C. Yu, R. J. Denman and W. Zhang, *Chem. Soc. Rev.*, 2013, **42**, 6634-6654.
19. J. R. Nitschke, *Chem. Soc. Rev.*, 2014, **43**, 1798-1799.
20. A. Wilson, G. Gasparini and S. Matile, *Chem. Soc. Rev.*, 2014, **43**, 1948-1962.
21. G. Gasparini, M. D. Molin, A. Lovato and L. J. Prins, 2012 Dynamic Covalent Chemistry Supramolecular Chemistry: From Molecule to Nanomaterials
22. C. Price, M. R. Elsegood, W. Clegg, N. H. Rees and A. Houlton, *Angew. Chem. Int. Ed.*, 1997, **36**, 1762-1764.
23. D. Amantia, C. Price, M. A. Shipman, M. R. Elsegood, W. Clegg and A. Houlton, *Inorg. Chem.*, 2003, **42**, 3047-3056.
24. J. Costamagna, J. Vargas, R. Latorre, A. Alvarado and G. Mena, *Coord. Chem. Rev.*, 1992, **119**, 67-88.
25. J. M. McCord and I. Fridovich, *J. Biol. Chem.*, 1969, **244**, 6049-6055.
26. H. Nozaki, H. Takaya, S. Moriuti and R. Noyori, *Tetrahedron*, 1968, **24**, 3655-3669.
27. A. B. Cohen, *Biochimica et Biophysica Acta (BBA)-Enzymology* 1975, **391**, 193-200.
28. P. A. Vigato and S. Tamburini, *Coord. Chem. Rev.*, 2004, **248**, 1717-2128.
29. N. Ledoux, R. Drozdak, B. Allaert, A. Linden, P. Van Der Voort and F. Verpoort, *Dalton Trans.*, 2007, 5201-5210.
30. S. Monsaert, N. Ledoux, R. Drozdak and F. Verpoort *J. Mol. Cat ; Chem A*. 2006, **260**, 221-226.
31. N. Ledoux, B. Allaert, D. Schaubroeck, S. Monsaert, R. Drozdak, F. Verpoort. *J Polym Sci Part A: Polym Chem.*, 2010, **48**, 302-310.
32. A. M. Lozano Vila, S. Monsaert, R. Drozdak, S. Wolowiec and F. Verpoort. *Adv. Synth. Cat.*; 2009, **351**, 2689-2701.
33. C. Jayabalakrishnan and K. Natarajan, *Transition Met. Chem.*, 2002, **27**, 75-79.
34. L.-A. H. Allen, L. S. Schlesinger and B. Kang, *J. Exp. Med.*, 2000, **191**, 115-128.
35. M. Aviram, E. Hardak, J. Vaya, S. Mahmood, S. Milo, A. Hoffman, S. Billicke, D. Draganov and M. Rosenblat, *Circulation* 2000, **101**, 2510-2517.
36. N. E. Borisova, M. D. Reshetova and Y. A. Ustynyuk, *Chem. Rev.* 2007, **107**, 46-79.

37. K. Osowska and O. Š. Miljanić, *Synlett*, 2011, **12**, 1643-1648.
38. M. M. Safont-Sempere, G. Fernandez and F. Würthner, *Chem. Rev.*, 2011, **111**, 5784-5814.
39. K. Osowska and O. Š. Miljanić, *J. Am. Chem. Soc.*, 2011, **133**, 724-727.
40. K. Osowska and O. Š. Miljanić, *Angew. Chem. Int. Ed.*, 2011, **50**, 8345-8349.
41. K. Acharyya and P. S. Mukherjee, *Chem. Commun.*, 2015, **51**, 4241-4244.
42. K. S. Chichak, S. J. Cantrill, A. R. Pease, S.-H. Chiu, G. W. Cave, J. L. Atwood and J. F. Stoddart, *Science* 2004, **304**, 1308-1312.
43. C. D. Pentecost, K. S. Chichak, A. J. Peters, G. W. Cave, S. J. Cantrill and J. F. Stoddart, *Angew. Chem. Int. Ed.* 2007, **46**, 218-222.
44. C. D. Meyer, C. S. Joiner and J. F. Stoddart, *Chem. Soc. Rev.*, 2007, **36**, 1705-1723.
45. P. C. Haussmann and J. F. Stoddart, *Chem. Rec.* 2009, **9**, 136-154.
46. Y. Liu, *Lawrence Berkeley National Laboratory* 2009.
47. G. Koshkaryan, D. Cao, L. M. Klivansky, S. J. Teat, J. L. Tran and Y. Liu, *Org. Lett.*, 2010, **12**, 1528-1531.
48. P. T. Glink, A. I. Oliva, J. F. Stoddart, A. J. White and D. J. Williams, *Angew. Chem.*, 2001, **113**, 1922-1927.
49. K. Bowman-James, *Acc. Chem. Res.*, 2005, **38**, 671-678.
50. D. J. Tranchemontagne, Z. Ni, M. O'Keeffe and O. M. Yaghi, *Angew. Chem. Int. Ed.*, 2008, **47**, 5136-5147.
51. J. W. Steed, J. L. Atwood, *Supramolecular chemistry*, John Wiley & Sons: West Sussex, U.K., 2000.
52. F. A. Cotton, C. Lin and C. A. Murillo, *Proc. Natl. Acad. Sci.*, 2002, **99**, 4810-4813.
53. F. A. Cotton, C. Lin and C. A. Murillo, *Acc. Chem. Res.*, 2001, **34**, 759-771.
54. M. Fujita, K. Umemoto, M. Yoshizawa, N. Fujita, T. Kusukawa and K. Biradha, *Chem. Commun.*, 2001, 509-518.
55. K. Harris, D. Fujita and M. Fujita, *Chem. Commun.*, 2013, **49**, 6703-6712.
56. J. K. Clegg, F. Li, K. A. Jolliffe, G. V. Meehan and L. F. Lindoy, *Chem. Commun.*, 2011, **47**, 6042-6044.
57. D. J. Bray, J. K. Clegg, L. F. Lindoy and D. Schilter, *Adv. Inorg. Chem.*, 2006, **59**, 1-37.

58. J. K. Clegg, L. F. Lindoy, B. Moubaraki, K. S. Murray and J. C. McMurtrie, *Dalton Trans.*, 2004, 2417-2423.
59. C. G. Oliveri, P. A. Ulmann, M. J. Wiester and C. A. Mirkin, *Acc. Chem. Res.*, 2008, **41**, 1618-1629.
60. N. C. Gianneschi, M. S. Masar and C. A. Mirkin, *Acc. Chem. Res.*, 2005, **38**, 825-837.
61. J. R. Nitschke, *Acc. Chem. Res.*, 2007, **40**, 103-112.
62. M. M. Smulders, I. A. Riddell, C. Browne and J. R. Nitschke, *Chem. Soc. Rev.*, 2013, **42**, 1728-1754.
63. T. K. Ronson, S. Zarra, S. P. Black and J. R. Nitschke, *Chem. Commun.*, 2013, **49**, 2476-2490.
64. D. Caulder and K. Raymond, *J. Am. Chem. Soc., Dalton Trans.* 1999, 1185-1200.
65. D. L. Caulder and K. N. Raymond, *Acc. Chem. Res.*, 1999, **32**, 975-982.
66. M. D. Pluth, R. G. Bergman and K. N. Raymond, *Acc. Chem. Res.*, 2009, **42**, 1650-1659.
67. B. H. Northrop, D. Chercka and P. J. Stang, *Tetrahedron* 2008, **64**, 11495-11503.
68. S. R. Seidel and P. J. Stang, *Acc. Chem. Res.*, 2002, **35**, 972-983.
69. S. Leininger, B. Olenyuk and P. J. Stang, *Chem. Rev.*, 2000, **100**, 853-908.
70. R. Chakrabarty, P. S. Mukherjee and P. J. Stang, *Chem. Rev.*, 2011, **111**, 6810-6918.
71. T. R. Cook, Y.-R. Zheng and P. J. Stang, *Chem. Rev.*, 2013, **113**, 734-777.
72. T.R. Cook and P.J. Stang, *Chem. Rev.*; (2015), DOI: 10.1021/cr5005666.
73. R. W. Saalfrank, H. Maid and A. Scheurer, *Angew. Chem. Int. Ed.*, 2008, **47**, 8794-8824.
74. R. W. Saalfrank, A. Stark, K. Peters and H. G. von Schnering, *Angew. Chem. Int. Ed.*, 1988, **27**, 851-853.
75. M. D. Ward, *Chem. Commun.*, 2009, 4487-4499.
76. M. D. Ward and P. R. Raithby, *Chem. Soc. Rev.*, 2013, **42**, 1619-1636.
77. Z. Lu, C. B. Knobler, H. Furukawa, B. Wang, G. Liu and O. M. Yaghi, *J. Am. Chem. Soc.*, 2009, **131**, 12532-12533.
78. H. Furukawa, K. E. Cordova, M. O'Keeffe and O. M. Yaghi, *Science* 2013, **341**, 1230444.
79. M. Li, D. Li, M. O'Keeffe and O. M. Yaghi, *Chem. Rev.*, 2013, **114**, 1343-1370.
80. W. Lu, Z. Wei, Z.-Y. Gu, T.-F. Liu, J. Park, J. Park, J. Tian, M. Zhang, Q. Zhang, T. Gentle III, M Bosch and HC Zhou, *Chem. Soc. Rev.*, 2014, **43**, 5561-5593.

81. J.-R. Li, D. J. Timmons and H.-C. Zhou, *J. Am. Chem. Soc.*, 2009, **131**, 6368-6369.
82. J.-R. Li and H.-C. Zhou, *Nat. Chem.*, 2010, **2**, 893-898.
83. J. R. Li and H. C. Zhou, *Angew. Chem. Int. Ed.*, 2009, **48**, 8465-8468.
84. J. R. Li, J. Yu, W. Lu, L-B Sun, J. Sculley, P. B. Balbuena and H. C. Zhou., *Nat. Commun.*, 2013, **4**, 1538.
85. M. D. Young, Q. Zhang and H.-C. Zhou, *Inorg. Chim. Acta.* 2015, **424**, 216-220.
86. S. De, K. Mahata and M. Schmittel, *Chem. Soc. Rev.*, 2010, **39**, 1555-1575.
87. N. J. Young and B. P. Hay, *Chem. Commun.*, 2013, **49**, 1354-1379.
88. N. Ahmad, A.H. Chughtai, H.A. Younus and F. Verpoort, *Coord. Chem. Rev.*, 2014, **280**, 1-27.
89. C. Piguet, M. Borkovec, J. Hamacek and K. Zeckert, *Coord. Chem. Rev.*, 2005, **249**, 705-726.
90. J. J. Perry Iv, J. A. Perman and M. J. Zaworotko, *Chem. Soc. Rev.*, 2009, **38**, 1400-1417.
91. A. Mishra and R. Gupta, *Dalton Trans.*, 2014, **43**, 7668-7682.
92. H. Vardhan and F. Verpoort, *Adv. Synth & Catal*, 2015, **357**, 1351-1368. .
93. M. Yoshizawa, J. K. Klosterman and M. Fujita, *Angew. Chem. Int. Ed.*, 2009, **48**, 3418-3438.
94. H.-N. Wang, X. Meng, G.-S. Yang, X.-L. Wang, K.-Z. Shao, Z.-M. Su and C.-G. Wang, *Chem. Commun.*, 2011, **47**, 7128-7130.
95. N.Ahmad, H.A. Younus, A.H. Chughtai and F. Verpoort, *Chem. Soc. Rev.*, 2015, **44**, 9-25.
96. A. Mallick, B. Garai, D. D. Díaz and R. Banerjee, *Angew. Chem.*, 2013, **125**, 14000-14004.
97. T.R. Cook, V. Vajpayee, M.H. Lee, P.J. Stang and K-W. Chi, *Acc. Chem. Res.*, 2013, **46**, 2464-2474.
98. Y.R. Zheng, K. Suntharalingam, T.C. Jhonstone and S.J. Lippard, *Chem. Sci.*, 2015, **6**, 1189-1193.
99. Y.-C. He, J. Yang, W.-Q. Kan and J.-F. Ma, *CrystEngComm* 2013, **15**, 848-851.
100. G. H. Ning, Y. Inokuma and M. Fujita, *Chem. Asian J.* 2013, **8**, 2596-2599.
101. A. Dubey, A. Mishra, J. W. Min, M. H. Lee, H. Kim, P. J. Stang and K.-W. Chi, *Inorg. Chim. Acta.*, 2014, **423**, 326-331.
102. A. Mishra, S. Ravikumar, Y. H. Song, N. S. Prabhu, H. Kim, S. H. Hong, S. Cheon, J. Noh and K.-W. Chi, *Dalton Trans.*, 2014, **43**, 6032-6040.
103. C. D. Meyer, C. Steven and J. F. Stoddart, *Chem. Soc. Rev.*, 2007, **36**, 1705-1723.

104. M. E. Belowich and J. F. Stoddart, *Chem. Soc. Rev.*, 2012, **41**, 2003-2024.
105. J. Sun and R. Warmuth, *Chem. Commun.*, 2011, **47**, 9351-9353.
106. P. Skowronek and J. Gawronski, *Org. Lett.*, 2008, **10**, 4755-4758.
107. T. Tozawa, J. T. Jones, S. I. Swamy, S. Jiang, D. J. Adams, S. Shakespeare, R. Clowes, D. Bradshaw, T. Hasell and S. Y. Chong, *Nat. Mat.* 2009, **8**, 973-978.
108. P. Mal, D. Schultz, K. Beyeh, K. Rissanen and J. R. Nitschke, *Angew. Chem.*, 2008, **120**, 8421-8425.
109. M. M. Smulders and J. R. Nitschke, *Chem. Sci.*, 2012, **3**, 785-788.
110. P. Mal, B. Breiner, K. Rissanen and J. R. Nitschke, *Science* 2009, **324**, 1697-1699.
111. I. A. Riddell, M. M. Smulders, J. K. Clegg and J. R. Nitschke, *Chem. Commun.*, 2011, **47**, 457-459.
112. T. K. Ronson, C. Giri, N. Kodiah Beyeh, A. Minkinen, F. Topić, J. J. Holstein, K. Rissanen and J. R. Nitschke, *Chem. Eur. J.* 2013, **19**, 3374-3382.
113. A. G. Salles Jr, S. Zarra, R. M. Turner and J. R. Nitschke, *J. Am. Chem. Soc.*, 2013, **135** (51), 19143-19146.
114. W. Meng, J. K. Clegg, J. D. Thoburn and J. R. Nitschke, *J. Am. Chem. Soc.*, 2011, **133**, 13652-13660.
115. J. L. Bolliger, A. M. Belenguier and J. R. Nitschke, *Angew. Chem. Int. Ed.*, 2013, **52**, 7958-7962.
116. R. A. Bilbeisi, J. K. Clegg, N. Elgrishi, X. d. Hatten, M. Devillard, B. Breiner, P. Mal and J. R. Nitschke, *J. Am. Chem. Soc.*, 2012, **134** (11), 5110-5119.
117. A. Jiménez, R. A. Bilbeisi, T. K. Ronson, S. Zarra, C. Woodhead and J. R. Nitschke, *Angew. Chem. Int. Ed.*, 2014, **53**, 4556-4560.
118. Y. R. Hristova, M. M. Smulders, J. K. Clegg, B. Breiner and J. R. Nitschke, *Chem. Sci.*, 2011, **2**, 638-641.
119. S. Ma, M. M. Smulders, Y. R. Hristova, J. K. Clegg, T. K. Ronson, S. Zarra and J. R. Nitschke, *J. Am. Chem. Soc.*, 2013, **135** (15), 5678-5684.
120. J. Mosquera, S. Zarra and J. R. Nitschke, *Angew. Chem. Int. Ed.*, 2014, **53**, 1556-1559.
121. N. Ousaka, S. Grunder, A. M. Castilla, A. C. Whalley, J. F. Stoddart and J. R. Nitschke, *J. Am. Chem. Soc.*, 2012, **134** (37), 15528-15537.
122. S. Zarra, D. M. Wood, D. A. Roberts and J. R. Nitschke, *Chem. Soc. Rev.*, 2015, **44**, 419-432.



123. A. J. McConnell, C. S. Wood, P. P. Neelakandan and J. R. Nitschke, *Chem. Rev.*, DOI: 10.1021/cr500632f.
124. T. K. Ronson, A. B. League, L. Gagliardi, C. J. Cramer and J. R. Nitschke, *J. Am. Chem. Soc.*, 2014, **136**, 15615-15624.
125. Y. Liu, X. Wu, C. He, Y. Jiao and C. Duan, *Chem. Commun.*, 2009, 7554-7556.
126. J. Wang, C. He, P. Wu, J. Wang and C. Duan, *J. Am. Chem. Soc.*, 2011, **133** (32), 12402-12405.
127. Y. Jiao, J. Wang, P. Wu, L. Zhao, C. He, J. Zhang and C. Duan, *Chem. Eur. J.* 2014, **20**, 2224-2231.
128. C. He, J. Wang, P. Wu, L. Jia, Y. Bai, Z. Zhang and C. Duan, *Chem. Commun.*, 2012, **48**, 11880-11882.
129. C. He, J. Wang, L. Zhao, T. Liu, J. Zhang and C. Duan, *Chem. Commun.*, 2013, **49**, 627-629.
130. L. Zhao, Y. Chu, C. He and C. Duan, *Chem. Commun.*, 2014, **50**, 3467-3469.
131. Y. Liu, Z. Lin, C. He, L. Zhao and C. Duan, *Dalton Trans.*, 2010, **39**, 11122-11125.
132. M. H. Alkordi, J. L. Belof, E. Rivera, L. Wojtas and M. Eddaoudi, *Chem. Sci.*, 2011, **2**, 1695-1705.
133. C. Browne, S. Brenet, J. K. Clegg and J. R. Nitschke, *Angew. Chem.*, 2013, **52**, 1944-1948.
134. C. He, Z. Lin, Z. He, C. Duan, C. Xu, Z. Wang and C. Yan, *Angew. Chem.*, 2008, **47**, 877-881.
135. Y. Liu, X. Wu, C. He, Z. Li and C. Duan, *Dalton Trans.*, 2010, **39**, 7727-7732.
136. M. Mazik, H. Cavga and P. G. Jones, *J. Am. Chem. Soc.*, 2005, **127** (25), 9045-9052.
137. H. Abe, Y. Aoyagi and M. Inouye, *Org. Lett.*, 2005, **7** (1), 59-61.
138. C. Schmuck and M. Schwegmann, *Org. Lett.*, 2005, **7** (16), 3517-3520.
139. M. M. J. Smulders, A. Jiménez and J. R. Nitschke, *Angew. Chem. Int. Ed.*, 2012, **51**, 6681-6685; *Angew. Chem.*, 2012, **124**, 6785-6789.
140. W. J. Ramsay, F. T. Szczypiński, H. Weissman, T. K. Ronson, M. M. J. Smulders, B. Rybtchinski and J. R. Nitschke, *Angew. Chem. Int. Ed.*, 2015, **54**, 5636-5640.
141. D. Li, Q. Feng, X.-L. Feng and J.-W. Cai, *Inorg. Chem. Commun.*, 2003, **6**, 361-364.
142. G. Jayamurugan, D. A. Roberts, T. K. Ronson, and J. R. Nitschke, *Angew. Chem. Int. Ed.*, 2015, **54**, 7539-7543.
143. R. A. Bilbeisi, T. K. Ronson and J. R. Nitschke, *Angew. Chem.*, 2013, **125**, 9197-9200.
144. Y. Jin, B. A. Voss, R. D. Noble and W. Zhang, *Angew. Chem.*, 2010, **122**, 6492-6495.

145. M. Mastalerz, M. W. Schneider, I. M. Oppel and O. Presly, *Angew. Chem. Int. Ed.*, 2011, **50**, 1046-1051.
146. F. J. Uribe-Romo, J. R. Hunt, H. Furukawa, C. Klöck, M. O’Keeffe and O. M. Yaghi, *J. Am. Chem. Soc.*, 2009, **131** (13), 4570-4571.
147. F. J. Uribe-Romo, C. J. Doonan, H. Furukawa, K. Oisaki and O. M. Yaghi, *J. Am. Chem. Soc.*, 2011, **133** (30), 11478-11481.
148. S.-Y. Ding, J. Gao, Q. Wang, Y. Zhang, W.-G. Song, C.-Y. Su and W. Wang, *J. Am. Chem. Soc.*, 2011, **133** (49), 19816-19822.
149. P. Pandey, A. P. Katsoulidis, I. Eryazici, Y. Wu, M. G. Kanatzidis and S. T. Nguyen, *Chem. Mater.*, 2010, **22** (17), 4974-4979.
150. H. Wang, W. Cao, T. Liu, C. Duan and J. Jiang, *Chem. Eur. J.* 2013, **19**, 2266-2270.
151. L. Zhao, Y. Liu, C. He, J. Wang and C. Duan, *Dalton Trans.*, 2014, **43**, 335-343.
152. A-M. Stadler, C. Burg, J. Ramirez and J.-M Lehn, *Chem. Commun.*, 2013, **49**, 5733-5735.
153. J.-P. Gisselbrecht, M. Gross, J.-M. Lehn, J.-P. Sauvage, R. Ziessel, C. Piccinni-Leopardi, J. M. Arrieta, G. Germain and M. V. Meersche, *Nouv. J. Chim.*, 1984, **8**, 661-667.
154. V. Amendola, L. Fabbri, P. Pallavivini, E. Sartirana and A. Taglietti, *Inorg. Chem.*, 2003, **42**, 1632-1636.
155. S. Hiraoka, Y. Sakata and M. Shinoya, *J. Am. Chem. Soc.*, 2008, **130**, 10058-10059.
156. H. Dong, J. Yang, X. Liu and S. Gou, *Inorg. Chem.*, 2008, **47**, 2913-2915.
157. J. Ramirez, A. M. Stadler, N. Kyritsakas and J.-M. Lehn, *Chem. Commun.*, 2007, 237-239.
158. P. J. Lusby, P. Müller, S. J. Pike and A. M. Z. Slawin, *J. Am. Chem. Soc.*, 2009, **131**, 16398-16400.
159. K. Parimal, E. H. Witlicki and A. H. Flood, *Angew. Chem. Int. Ed.*, 2010, **49**, 4628-4632.
160. S. Chen, L.-J. Chen, H.-B. Yang, H. Tian and W. Zhu, *J. Am. Chem. Soc.*, 2012, **134**, 13596-13599.